Attachment H – Factors to Consider in the Development of Water Column Monitoring Plans for Performance Standards

This Attachment describes analyses performed with contaminant fate and transport (CFT) model results to support development of monitoring plans for water column suspended sediment and contaminants which will provide a basis for assessing whether conditions during construction of the selected remedy are consistent with expected releases during dredging and identify time periods when corrective actions may be needed to bring construction performance back into the range of acceptable conditions. The CFT model results are based on simulations performed as part of the evaluation of alternatives to support the ROD, and include simulations for the Selected Remedy and the No Action Alternative[1].

The simulations performed for the active remedial alternatives involved running the model from 2013 (end of the calibration period) to July 2020 when construction was assumed to begin, then through the period of construction (December 2025 for the selected remedy) and for a period of 30 years after completion of construction. The hydrographs and tidal boundary conditions used for the alternatives were developed by repeating the model inputs (boundary inflows and tides) for the period October 1995 – October 2010 (water years 1996-2010) in 15-year cycles and appending them to the historical water year 1995 – 2013 inputs to generate one continuous simulation for the period of water years 1996 through 2064. The No Action alternative is identical to the active remedial alternatives up to July 2020, and uses the same hydrographs and tidal boundary conditions as the active alternatives, but does not include any remediation during the period of construction for the three active remedial alternatives. The No Action alternative also does not include any dredging to reestablish the navigation channel in the LPR. Results from the No Action alternative are used for comparison to results from the Selected Remedy, as described below.

Contaminant concentrations in the water column of the LPR at any point in time are affected by river flow and tidal conditions, the location and movement of the salt front (as an indicator of the estuarine turbidity maximum), and antecedent conditions (e.g. time since most-recent high flow condition). During the period of dredging, it is expected that contaminant concentrations will also be affected by unavoidable releases of sediment and contaminants related to the dredging activities, despite best efforts to minimize these construction related releases. Analyses were performed with CFT model simulation results in an attempt to characterize expected conditions, which could then be used to identify conditions outside the expected range and signal the need for corrective actions during construction activities.

Analyses described below provide information that can be considered in developing performance standards in terms of:

1. Water column contaminants concentrations,
2. Differences in concentration upstream and downstream of the dredging operation,
3. Contaminant mass transport across lateral transects.

Variations in Water Column Contaminant Concentrations with River Flow

[1] Details of these remedial alternatives (e.g. dredging and capping sequence and schedule, production rates, etc.) are presented in Appendix V (Responsiveness Summary) of the ROD (EPA, March 2016).

Water column concentrations of 2,3,7,8-TCDD computed over the simulation period of construction (water years 2020 – 2026) in the model layers representing the top 10 percent of the water column (Figure 1) and bottom 10 percent (Figure 2) are plotted versus fresh water flow at Dundee Dam, with different colors identifying results computed during periods of varying tidal velocities. The locations plotted on Figures 1 and 2 include the representative grid cells at approximately two mile intervals, which were shown in other attachments (e.g. A-1 ad A-2), and also include grid cells at bridge crossings, labeled as RM 8.0 and RM 1.2, which could potentially be used as fixed monitoring locations.

Concentrations of 2,3,7,8-TCDD decrease more significantly with increasing river flow at more-upstream locations (i.e top three panels) and less so at more-downstream locations (i.e. last three panels), in part because the increase in freshwater flow represents more of a dilution flow due to the relatively smaller 2,3,7,8-TCDD source from upstream. With increasing distance downstream, greater surface area of contaminated sediment results in additional sources of 2,3,7,8-TCDD, which offsets the dilution flow. Comparing Figures 1 and 2, shows concentrations in the bottom layer are higher than in the surface layer, but with similar relationships with river flow. At each location, the variation in concentration at any given river flow is generally 1 to 1.5 orders of magnitude. Identifying variations in concentration as a function of variations in tidal velocities is difficult because of the variability in concentrations over a range of tidal velocities. Concentrations of 2,3,7,8-TCDD versus river flow are presented for RM 8.1 (Figure 3) and RM 2 (Figure 4) with each panel showing the results from only one of the velocity ranges that are represented by different colors on the aggregate panel from Figure 1. Although some differences can be seen in comparing concentrations calculated within different tidal velocity ranges (i.e. different panels on Figures 3 and 4), at a given flow, there is overlap in concentrations over a wide range in tidal velocity.

Selected Remedy simulation results for water column 2,3,7,8-TCDD concentrations are presented on Figures 5 (surface layer) and Figure 6 (bottom layer) in a format consistent with results from the No Action simulation (Figures 1 and 2). (Note that the y-axis scales are different than Figures 1 and 2 to accommodate the higher maximum concentrations in the Selected Remedy simulation results.) 2,3,7,8-TCDD concentrations from the Selected Remedy simulations are higher than those from the No Actions simulation, although the 1 to 1.5 order of magnitude variation still exists at any river flow. This makes identifying an expected concentration at a specific river flow and tidal velocity very uncertain.

Spatial Patterns of Contaminant Concentrations During Dredging Period

Selected Remedy simulation results for water column 2,3,7,8-TCDD concentrations are presented as spatial profiles on a series of figures starting at Figure 7. The format of this series of figures includes a time-series of hourly tidal flow (volume flux) and water surface elevation (upper left panel) for a week before dredging, the period of dredging (tan shading), and a week following dredging of the selected grid cell. The map on the upper right indicates where dredging is simulated at the time corresponding to the vertical line shown within the upper left panel. The two large panels present spatial profiles of surface layer and bottom layer 2,3,7,8-TCDD concentrations in four model grid cells upstream and four grid cells downstream of the cell being dredged (vertical line in the lower two panels) at the time printed in the upper left of the middle panel and indicated by the vertical line shown within the upper left panel. The legend on the bottom left indicates the symbols used to identify model grid cells across the river at a given location, beginning with 16 on the west or southern shoreline and increasing laterally across the river. A circle surrounds the symbol corresponding to the deepest grid cell in each cross section. Each series includes spatial profiles at seven times:

1. Low slack tide

2. Flood tide 1 hour after low slack tide
3. Peak flood tide
4. High slack tide
5. Ebb tide 1 hour after high slack tide
6. Peak ebb tide
7. Low slack tide

Results for three of the seven locations shown on Figures 5 and 6 are presented as spatial profiles. Locations near RM 8 are not shown because concurrent dredging in multiple grid cells in that area complicates interpretation of the spatial profiles in that area. Locations downstream of RM 2 are not shown because the results at those locations show patterns similar to RM 2. For two of the three locations shown, the dredging duration is long enough to include periods of both spring and neap tides, and examples are shown for each.

RM 6.3 Neap Tide Conditions

Figures 7 – 13 present results at the time of dredging at RM 6.3 during a neap tide condition. At low slack tide (Figure 7) the peak concentration is located in the cell being dredged, which is typical throughout the river, due to ongoing releases from dredging with minimal dilution resulting from near-zero tidal velocities approaching slack tide. After an hour of flooding tide (Figure 8), concentrations upstream of the dredging locations are higher than downstream concentrations, but this gradient flattens out during peak flood conditions (Figure 9). During high slack tide (Figure 10), the concentration at the dredging location is higher than surrounding areas, however, it is noted that the concentrations are higher at the high slack than at the low slack (Figure 7). After an hour of ebbing tide (Figure 11) surface layer concentrations downstream of the dredging locations are higher than upstream locations. Similar to the peak flood conditions (Figure 9), during peak ebb conditions (Figure 12), the spatial gradients in concentration tend to flatten out before returning to the low ebb tide with the peak concentration at the dredging location (Figure 13).

RM 6.3 Spring Tide Conditions

As dredging continues at RM 6.3, conditions transition from neap to spring tides and peak tidal flows are approximately 50 percent higher that during the period shown on Figures 7 - 13. During low slack (Figure 14) the peak concentration at the dredging location is lower than during neap tide conditions (Figure 7) and concentrations downstream of the dredging location are higher than calculated during neap tide conditions. After an hour of flooding tide (Figure 15), surface layer concentrations upstream of the dredging location are slightly higher than downstream concentrations. In the bottom layer, there is a noticeable gradient, with the highest concentration at the most downstream location shown on Figure 15 and decreasing to the most upstream location (with the exception of the dredging location). The elevated concentrations downstream of the dredging location could be due to a combination of the cumulative effect releases of contaminants during the preceding 9 days, the effect of estuarine circulation carrying sorbed contaminants in the upstream direction as the freshwater flow decreased from over 3000 cfs at the beginning of January to almost 800 cfs on January 20th (Figure 15), as well as the increased tidal flows associated with the spring tide. It is noted that the peak tidal flow, above 27,000 cfs, is more that 30 times greater than freshwater flow of approximately 800 cfs at this time. At the peak flood condition (Figure 16) the spatial gradients flatten out, although at higher concentrations than calculated during the neap tide condition (Figure 9). At high slack tide (Figure 17) the peak concentration is located at the dredging location, and after an hour of ebbing flow (Figure 18) concentrations downstream of the dredging location are somewhat higher than upstream concentrations, but the difference is not as great as during neap tide conditions (Figure 11). During peak ebb

conditions (Figure 19) surface layer concentrations remain slightly elevated downstream of the dredging location relative to upstream, but bottom layer concentrations increase substantially from slack tide conditions are somewhat variable spatially. At low slack tide (Figure 20) the peak concentration is again located at the dredging location.

RM 4 Neap and Spring Tide Conditions

Figures 21 – 27 present results at the time of dredging at RM 4 following neap tide, but closer to the neap than the spring tide condition. (Note the change in the y-axis scale relative to the RM 6.3 plots, due to the high concentrations during slack tides at the dredging location at RM 4. At low slack tide (Figure 21) the peak concentration is again located in the cell being dredged, with downstream concentrations slightly elevated relative to upstream concentrations. After an hour of flooding tide (Figure 22), concentrations upstream of the dredging locations are higher than downstream concentrations, but this gradient flattens out during peak flood conditions (Figure 23). During high slack tide (Figure 24), the concentration at the dredging location is higher than surrounding areas; however, the concentrations downstream of the dredging location are higher than upstream concentrations. After an hour of ebbing tide (Figure 25) concentrations downstream of the dredging locations are higher than upstream of the dredging location. Similar to the peak flood conditions (Figure 23), during peak ebb conditions (Figure 26), the spatial gradients in concentration tend to flatten out before returning to the low ebb tide with the peak concentration at the dredging location (Figure 27).

Figures 28 – 34 present results at the time of dredging at RM 4 during Spring tide conditions. Much less difference is noted between the results during spring and neap tide conditions at RM 4 (compared to the differences noted at RM 6.3). Slack tide concentrations at the dredging location tend to be lower in the bottom layer during spring tide (Figure 28 versus Figure 21 and Figure 31 versus Figure 24), but otherwise the spatial profiles are fairly similar.

RM 2 Spring Tide Conditions

Water column concentrations of 2,3,7,8-TCDD at the time of dredging at RM 2 are shown on Figures 35-41. Dredging at this location is simulated during a low flow period, when flows at Dundee Dan are less than 200 cfs, and starts at a spring tide and transitions towards a neap tide. Dredging at this location is simulated approximately 8 weeks after the dredging program began, so the cumulative effect of releases of sediment and contaminants from other locations is more-limited than for areas dredged later in the program.

At RM 2, concentration gradients are relatively flat across the 0.8 mile section shown on Figures 35-41. The highest concentrations are calculated at low slack tide (Figure 25), indicating that higher concentrations are being transported from upstream to RM 2. After one hour of flooding tide (Figure 36) concentrations in the surface layer are similar to concentrations at low slack, and bottom layer concentrations of 2,3,7,8-TCDD are slightly elevated from the low slack profile. At peak flood conditions (Figure 37), concentrations in both the surface and bottom layer are noticeably lower than those on the two preceding figures, and a slight spatial gradient has developed with lower concentrations downstream and higher concentrations upstream. At high slack tide (Figure 38) concentration gradients are very flat and concentrations are at their minimum values, and very little change is noted after one hour of ebbing tide (Figure 39). At peak ebb tide (Figure 40) concentrations have risen somewhat and a slight spatial gradient is seen, with higher concentrations upstream and lower concentrations downstream. Conditions at low slack tide (Figure 41) again show relatively flat spatial profiles with concentrations elevated relative to the preceding

flood and ebb conditions.

Contaminant mass transport across lateral transects

Another option for monitoring during construction is to estimate contaminant fluxes in the water column passing through lateral transects. In order to quantify fluxes, both the tidal flow and the contaminant concentration in that water must be measured or estimated. There are obvious trade-offs in the accuracy of the flux estimate and the complexity of the program, such as number of monitoring points across the cross section and number of measurements per day or tidal cycle. Model results were used to explore the effect of measuring velocity and contaminant concentrations at only one monitoring location (the deepest point in the cross section was selected) to estimate the total advective contaminant flux through that cross section.

An important component of the flux estimate is the calculation of the water flow through the chosen cross section. If the estimate of the water flow through the cross section is not accurate, this will have a significant impact on the error in the calculated contaminant flux. If the flow is only measured in the location where the concentration sampling is done, it is necessary to obtain a relationship between the flow measured at that point and the flow through the whole cross section. This relationship could be developed during the pre-design investigation with vessel-mounted ADCP measurements across transects where monitoring will be conducted. Model results were used to illustrate this relationship by plotting the flow through all grid cells in a transect versus flow through only the deepest grid cell in the transect. The relationship varies with location, due to variations in cross section geometry and flow stratification, as can be seen by the difference between transects at RM 8.1 (Figure 42) and RM 1.2 (Figure 43). Although the relationships are different, linear relationships allow the transect-total flow to be estimated from the flow at the deepest grid cell. In addition to location-specific variations, these relationships also depend on the in-river conditions including position in the tidal cycle, position in the spring and neap cycle, high flow conditions, and other changes in the condition of the flow. Figure 44 includes a plot demonstrating variation of the flow relationship with spring and neap tidal conditions. In order to minimize error, the flow through the cross section must be measured in similar conditions to the conditions of interest. To obtain an accurate representation of the flow through the cross section, vessel-mounted Acoustic Doppler Current Profilers (ADCP) measurements across the width of the channel should be conducted at peak ebb and flood under several different magnitudes of fresh water inflow over Dundee Dam and at several points in the spring neap cycle.

Another major source of error in the calculation of contaminant flux is the estimation of the in-river contaminant concentration. The in-river concentration changes throughout each tidal cycle, and changes with the spring-neap cycle and other river conditions. More accurate flux estimates will be obtained with more-frequent contaminant measurements, and as the number of measurements per day are reduced based on practicality, some error will be introduced. Intra-tidal variations in flows are much greater than the computed intra-tidal variations in contaminant concentrations, as seen in Figures 7 – 41. Model results were used to test the accuracy of flux estimates made with contaminant concentrations sampled during the peak ebb and flood, since this is when the flows and thus the contaminant flux are largest. The largest error would be introduced by poor estimation of the contaminant concentration in the river during those periods of peak flows. The less often concentration measurements are done, the greater the potential error which will be introduced into the final contaminant flux calculation. Sampling at lower frequencies also introduces the potential to miss transient high concentration events which can result in spikes of contaminant flux. Figure 45 demonstrates an estimation of the contaminant flux compared to the calculated in-river flux from the model output, with an assumption of grab sampling roughly twice daily, once at peak flood and once at peak ebb. There are several points within the time span when errors in the predicted

contaminant flux are observed due to variations in the concentration with changes in river conditions. Figure 46 presents an estimation built on the same assumptions as Figure 45, but with sampling once daily, alternating between peak ebb and flood. The estimate of contaminant flux in Figure 46 compares poorly relative to the result shown in Figure 45, particularly in the later portion of the time series when as the concentration has some larger gradients in time. Figure 47 presents the time series of contaminant concentration during this period for reference.

It is important to note that reducing errors in the predicted gross fluxes will have a significant impact on the calculation of net flux as the net flux through a given cross section of the river is a small difference in much larger gross fluxes. This is particularly true if is there is a bias in the direction of the errors in the estimated gross fluxes. As an example, between hours 350 and 450 for Figure 45, the total gross contaminant flux error is roughly 7.3 percent, while the net contaminant flux error is roughly 43.9 percent. This is exacerbated by decreases in the frequency of concentration measurements as transient changes in concentration during a peak flood or ebb can throw the estimated net contaminant flux off by a significant margin. As an example, between hours 550 and 650 for Figure 45 the net contaminant flux error is roughly 46.3 percent, while the net contaminant flux error for Figure 46 is roughly 63.3 percent.

Conclusions

Calculated variations in contaminant concentrations of 1 to 1.5 order of magnitude at any river flow makes specification of a performance standard based on a single concentration, or a flow-based variable concentration a relatively ineffective option for ensuring that undesirable construction performance will be detected without incorrectly characterizing proper construction performance as unacceptable.

Use of differences in concentration from up-current to down-current (i.e. upstream versus downstream, considering the direction of the tidal flow) locations is a potential strategy for specifying performance standards, but would require that sampling be performed at carefully specified points in the tidal cycle to assess construction performance.

Calculation of contaminant fluxes passing lateral transects is a potential option which would require both fixed location monitoring and periodic vessel-mounted ADCPs surveys to allow limited-location velocity measurements to be used to estimate cross-sectional total flows. The accuracy in estimating contaminant concentrations to pair with intra-tidal flows can be improved with a more detailed contaminant monitoring program (i.e. increased frequency and increased number of cross-sectional points) but practical limitations need to be considered.

All of the analyses presented in this attachment that are based on model results from the Selected Remedy simulation, include the specification of the sediment and contaminant release rate of 3 percent of the dredged mass, which was adopted as a conservative assumption for the evaluation of alternatives. Limited additional model simulations with alternate releases rates in individual grid cells, to mimic poor or undesirable construction performance, may provide useful information to contrast the response of contaminant concentrations, spatial profiles and mass fluxes to deviations in construction performance with routine acceptable performance.

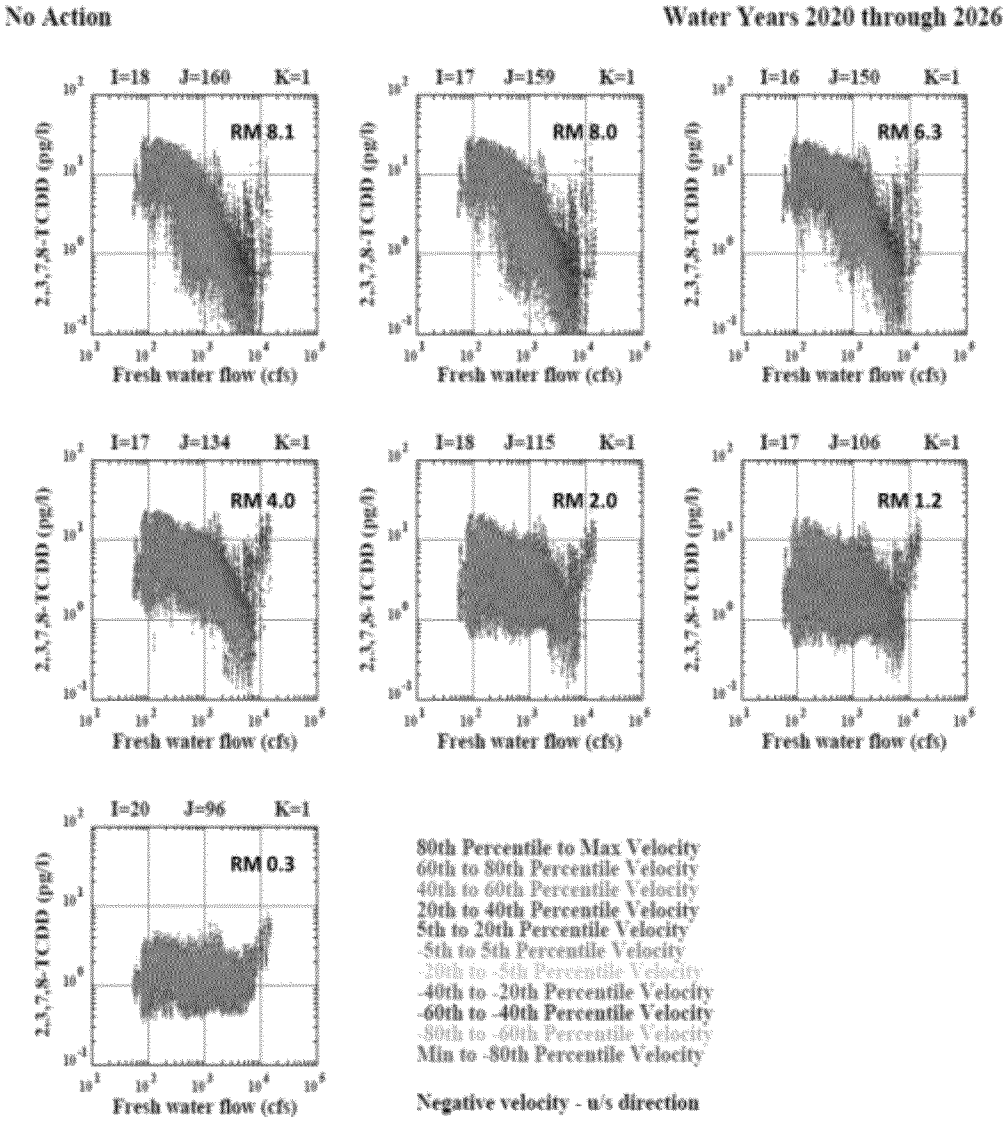

Surface layer water column concentrations of 2,3,7,8-TCDD versus River Flow at Dundee Dam, at representative locations from the No-Action simulation concentrations

Figure 1

Lower 8.3 Miles of the Lower Passaic River

2016

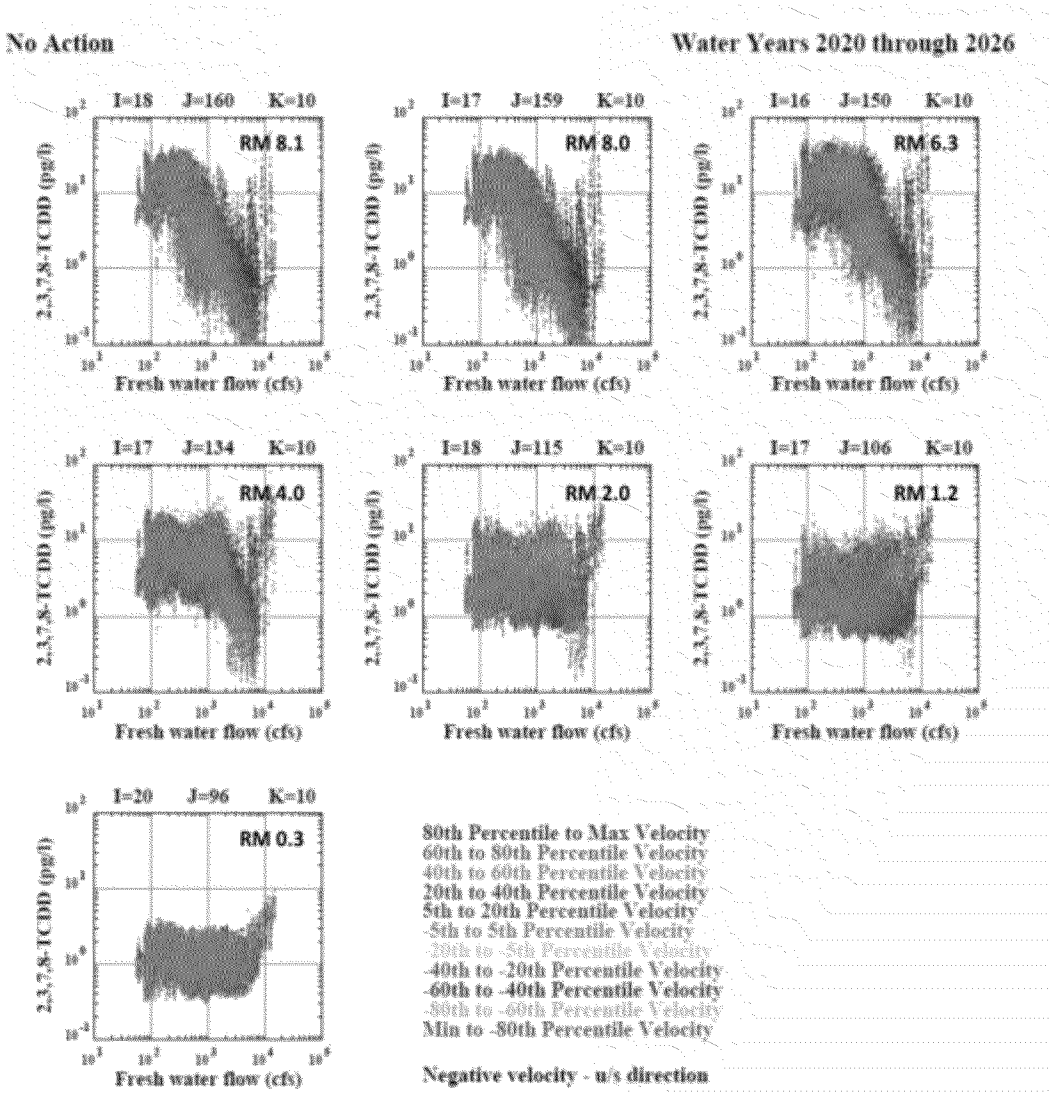

~~Bottom layer water column concentrations of 2,3,7,8-TCDD versus River Flow at~~ Dundee Dam, at representative locations from the No-Action simulation concentrations

Figure 2

Lower 8.3 Miles of the Lower Passaic River

2016

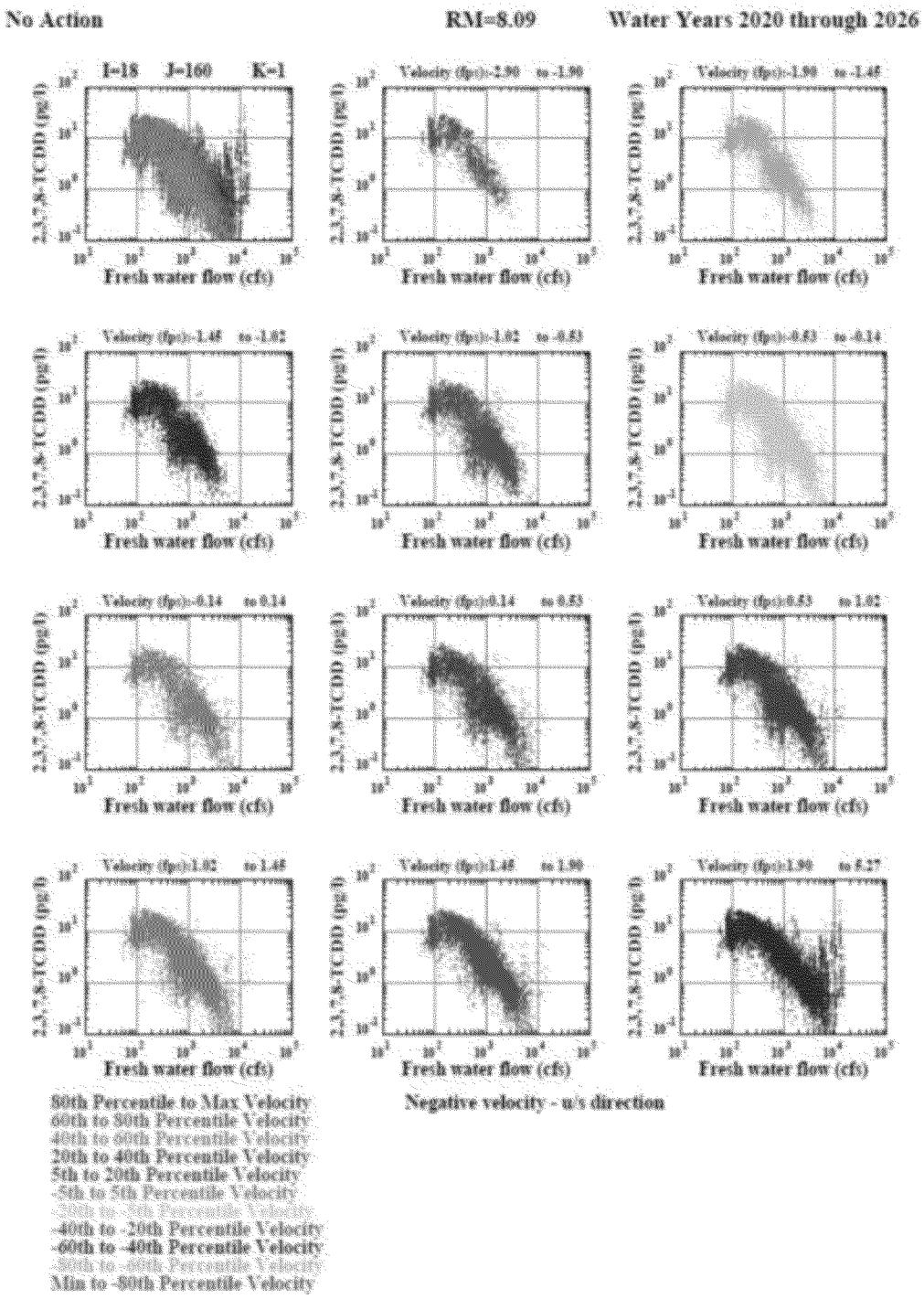

Surface layer water column concentrations of 2,3,7,8-TCDD versus River Flow at Dundee Dam, by tidal velocity range at RM 8.1 from the No-Action simulation concentrations

Figure 3

2016

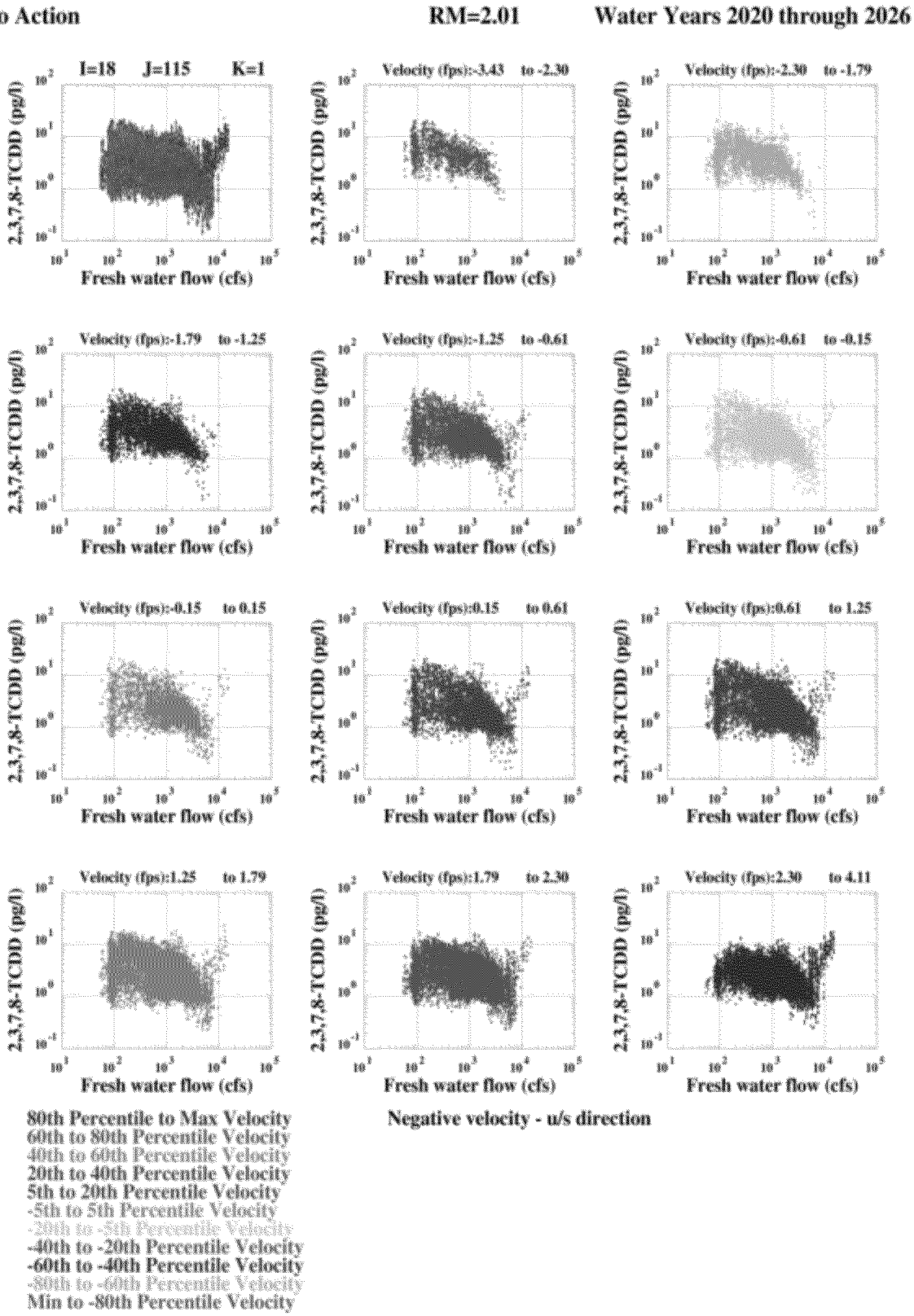

Surface layer water column concentrations of 2,3,7,8-TCDD versus River Flow at Dundee Dam, by tidal velocity range at RM 2.0 from the No-Action simulation concentrations

Figure 4

2016

Lower 8.3 Miles of the Lower Passaic River

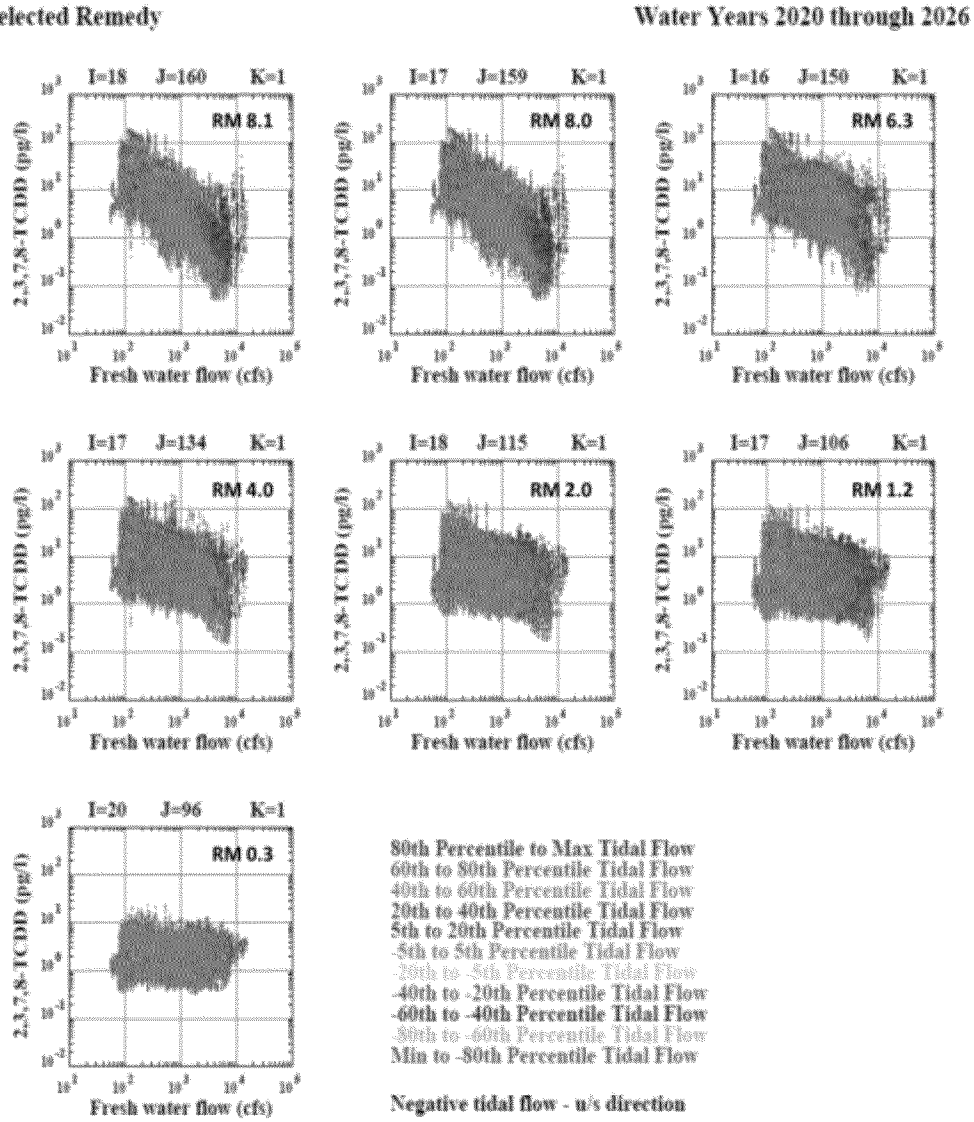

Surface layer water column concentrations of 2,3,7,8-TCDD versus River Flow at Dundee Dam, at representative locations from the Selected Remedy simulation concentrations

Figure 5

2016

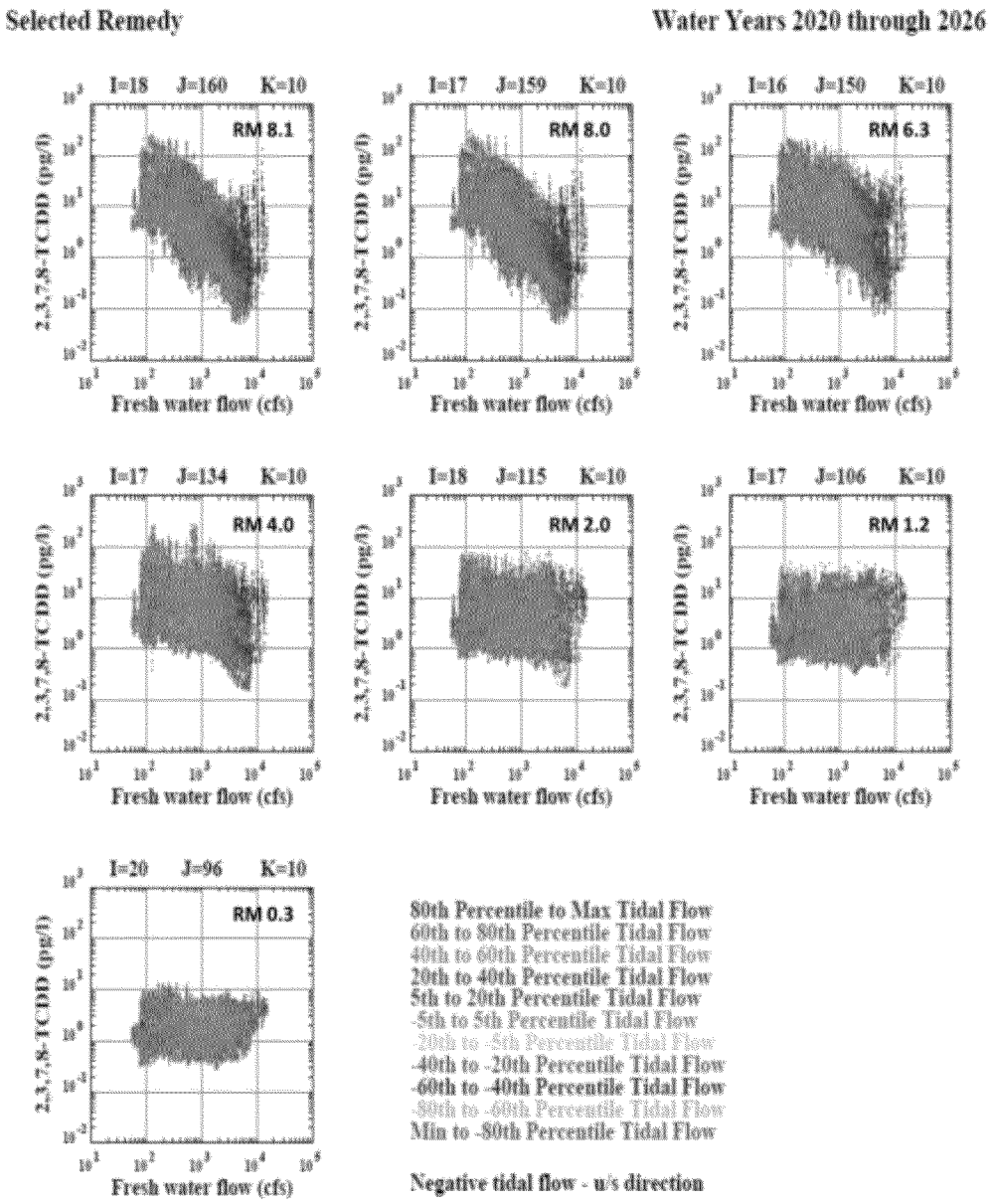

Bottom layer water column concentrations of 2,3,7,8-TCDD versus River Flow at Dundee Dam, at representative locations from the Selected Remedy simulation concentrations

Figure 6

2016

Lower 8.3 Miles of the Lower Passaic River

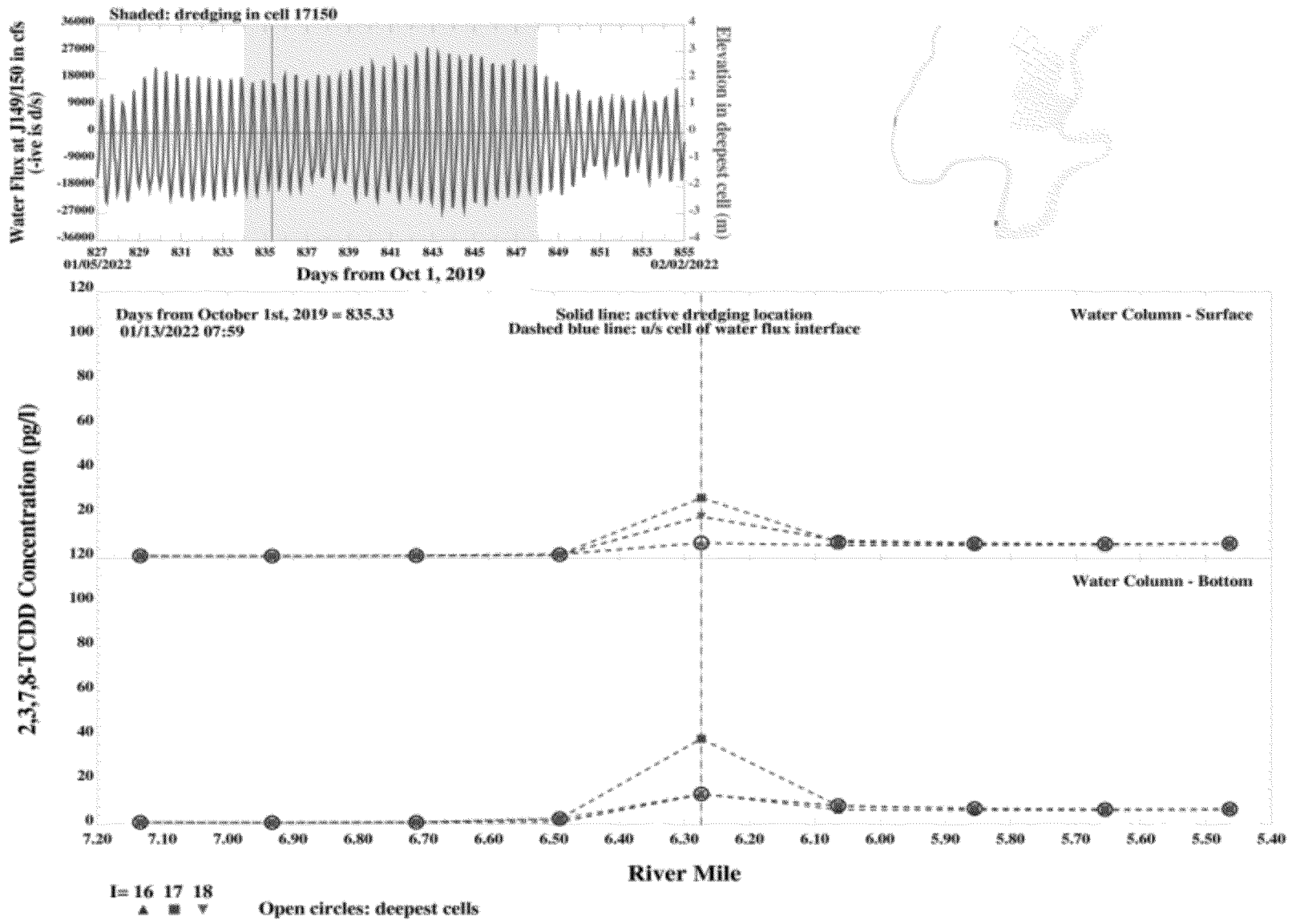

Spatial profile of 2,3,7,8-TCDD water column concentrations during dredging near RM 6.3 - neap tide - low slack tide

Figure 7

Lower 8.3 Miles of the Lower Passaic River

2016

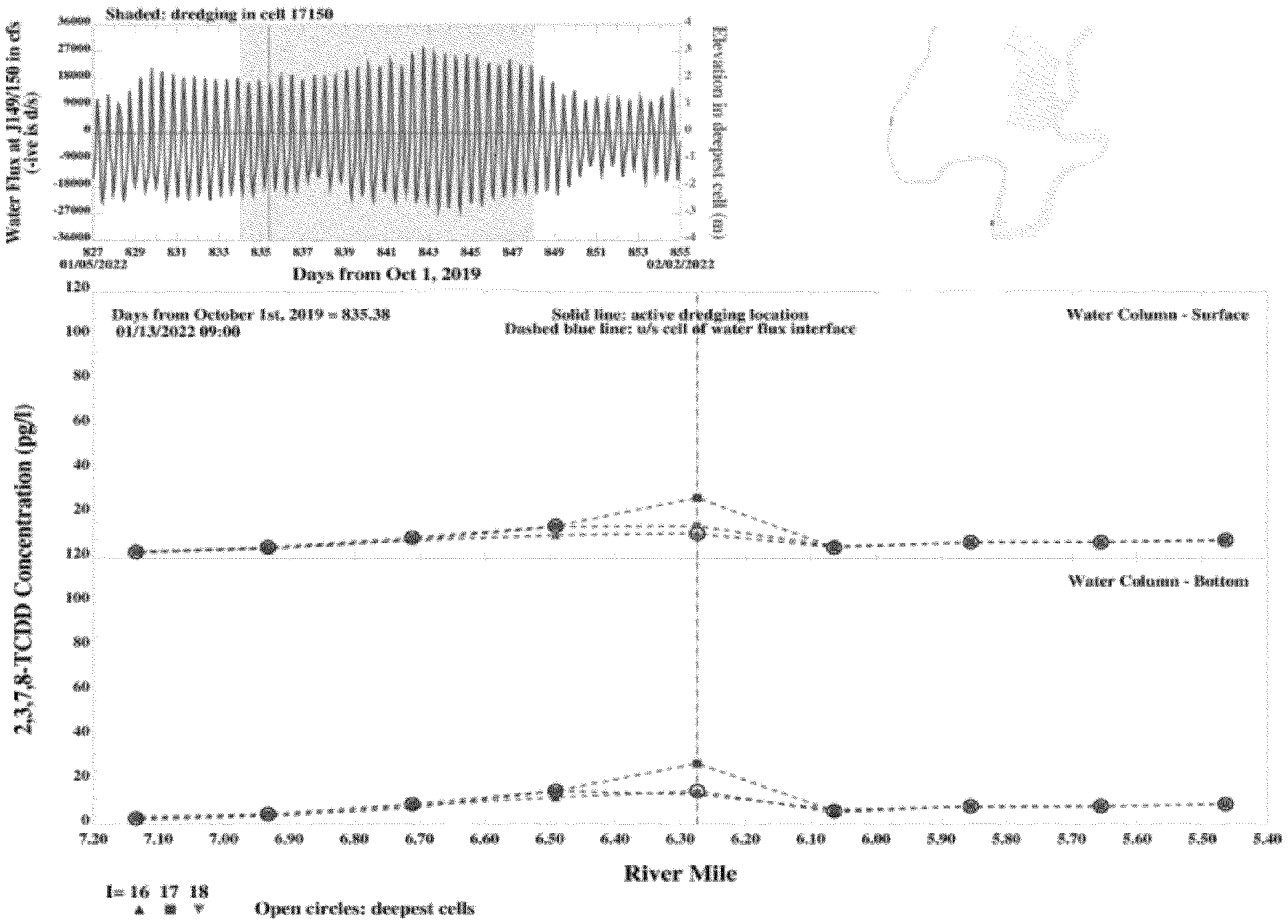

Spatial profile of 2,3,7,8-TCDD water column concentrations during dredging near RM 6.3 - neap tide - flood tide 1 hour after low slack tide

Figure 8

Lower 8.3 Miles of the Lower Passaic River

2016

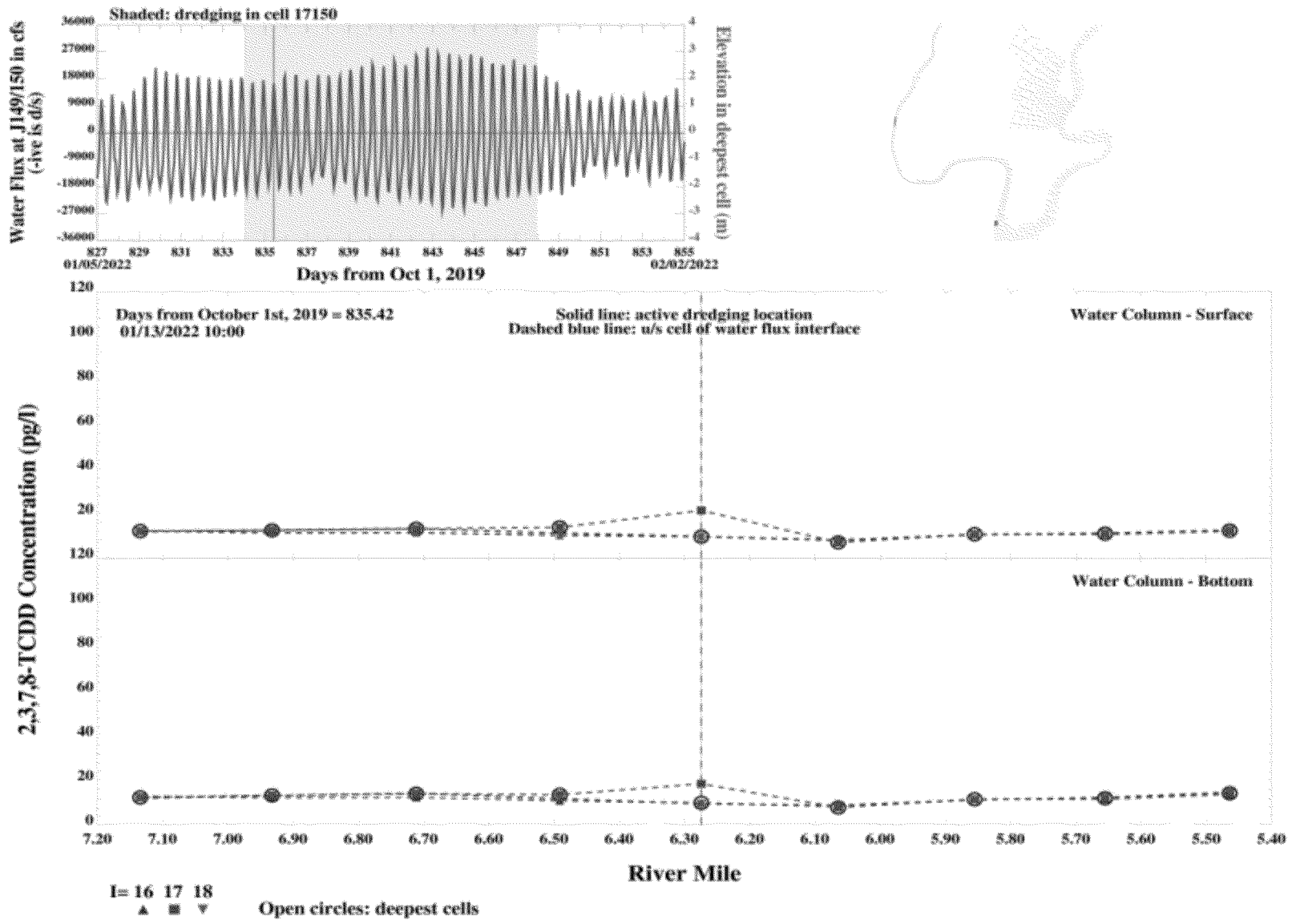

Spatial profile of 2,3,7,8-TCDD water column concentrations during dredging near RM 6.3 - neap tide - peak flood tide	Figure 9
Lower 8.3 Miles of the Lower Passaic River	2016

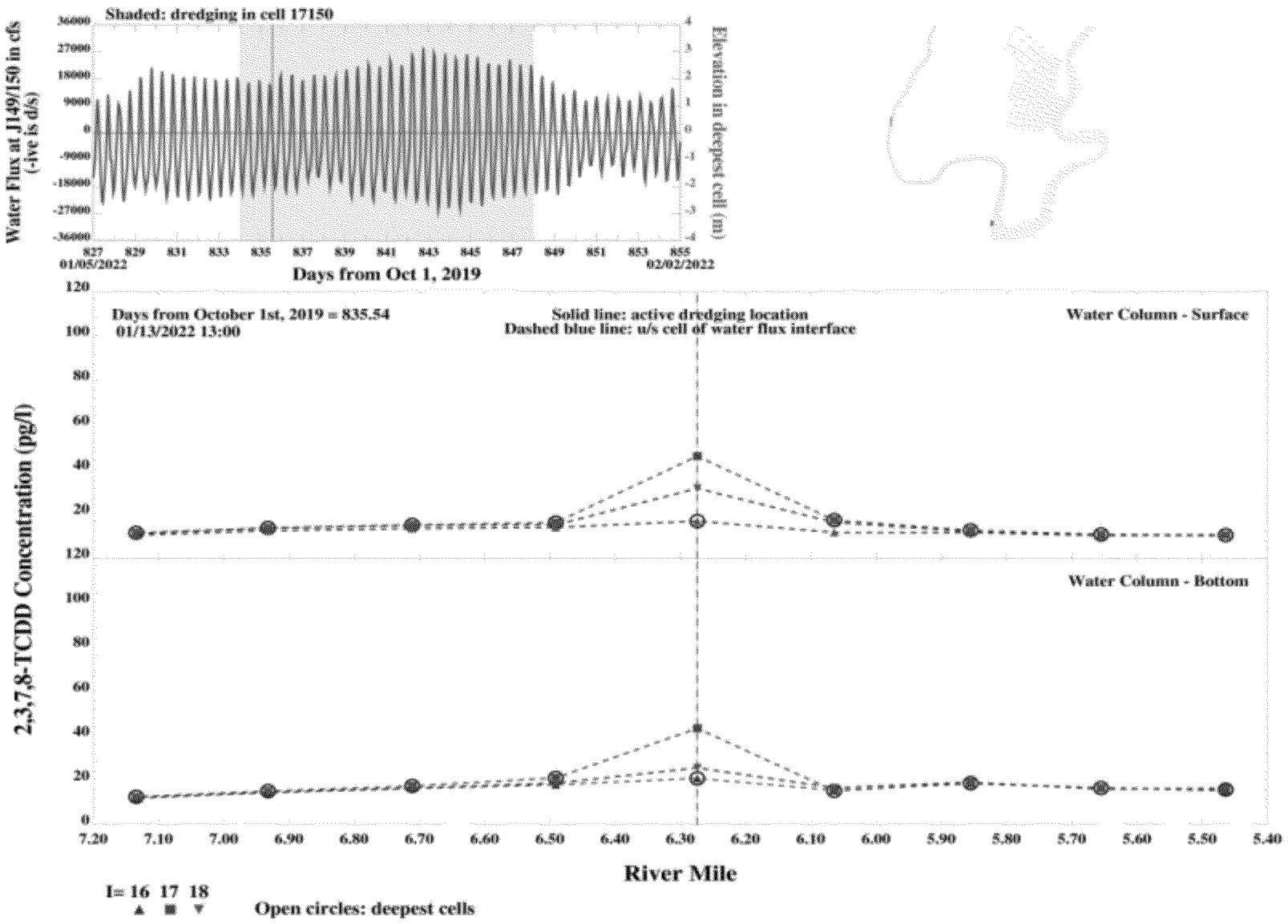

Spatial profile of 2,3,7,8-TCDD water column concentrations during dredging near RM 6.3 - neap tide - high slack tide

Figure 10

Lower 8.3 Miles of the Lower Passaic River

2016

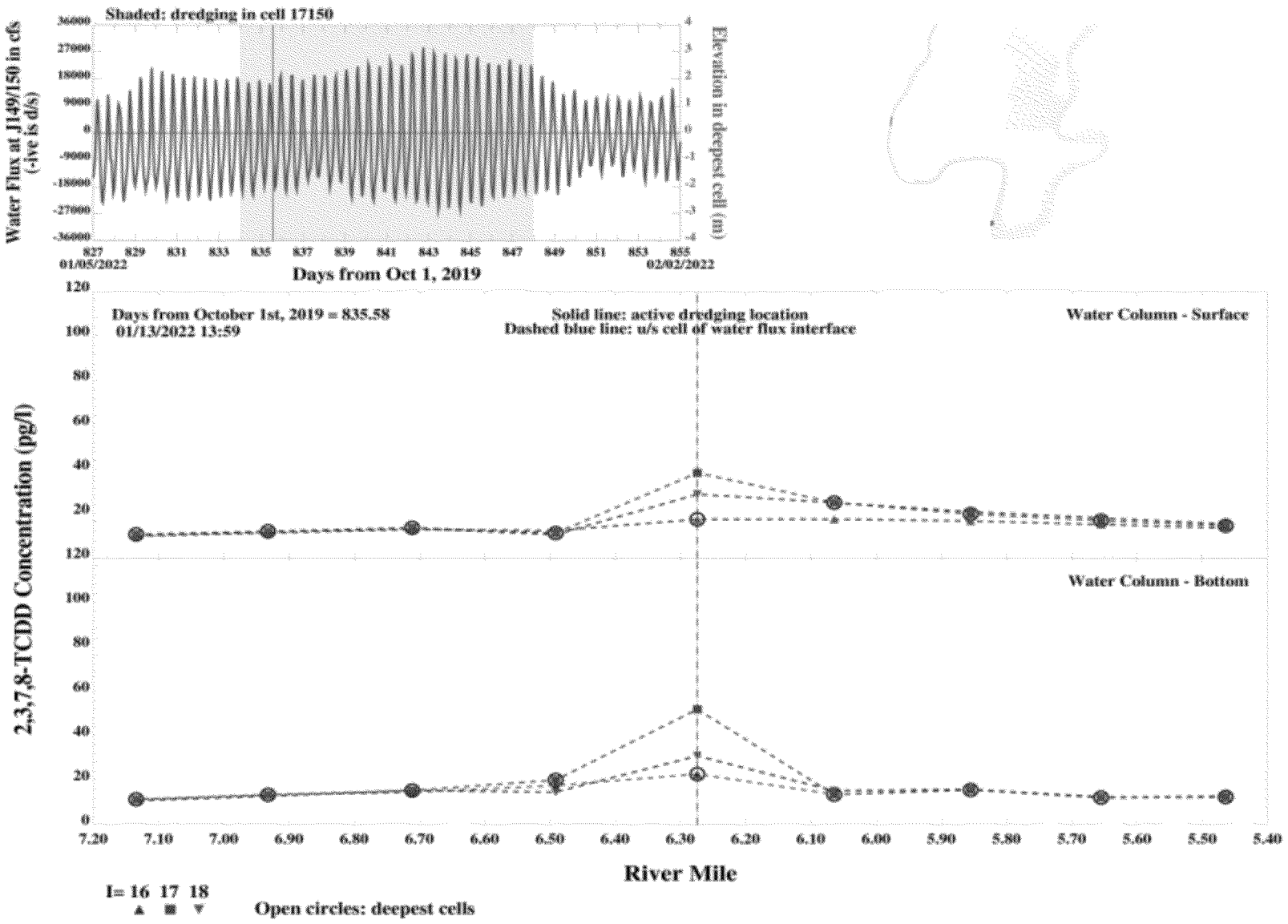

Spatial profile of 2,3,7,8-TCDD water column concentrations during dredging near RM 6.3 - neap tide - ebb tide 1 hour after high slack tide

Figure 11

Lower 8.3 Miles of the Lower Passaic River

2016

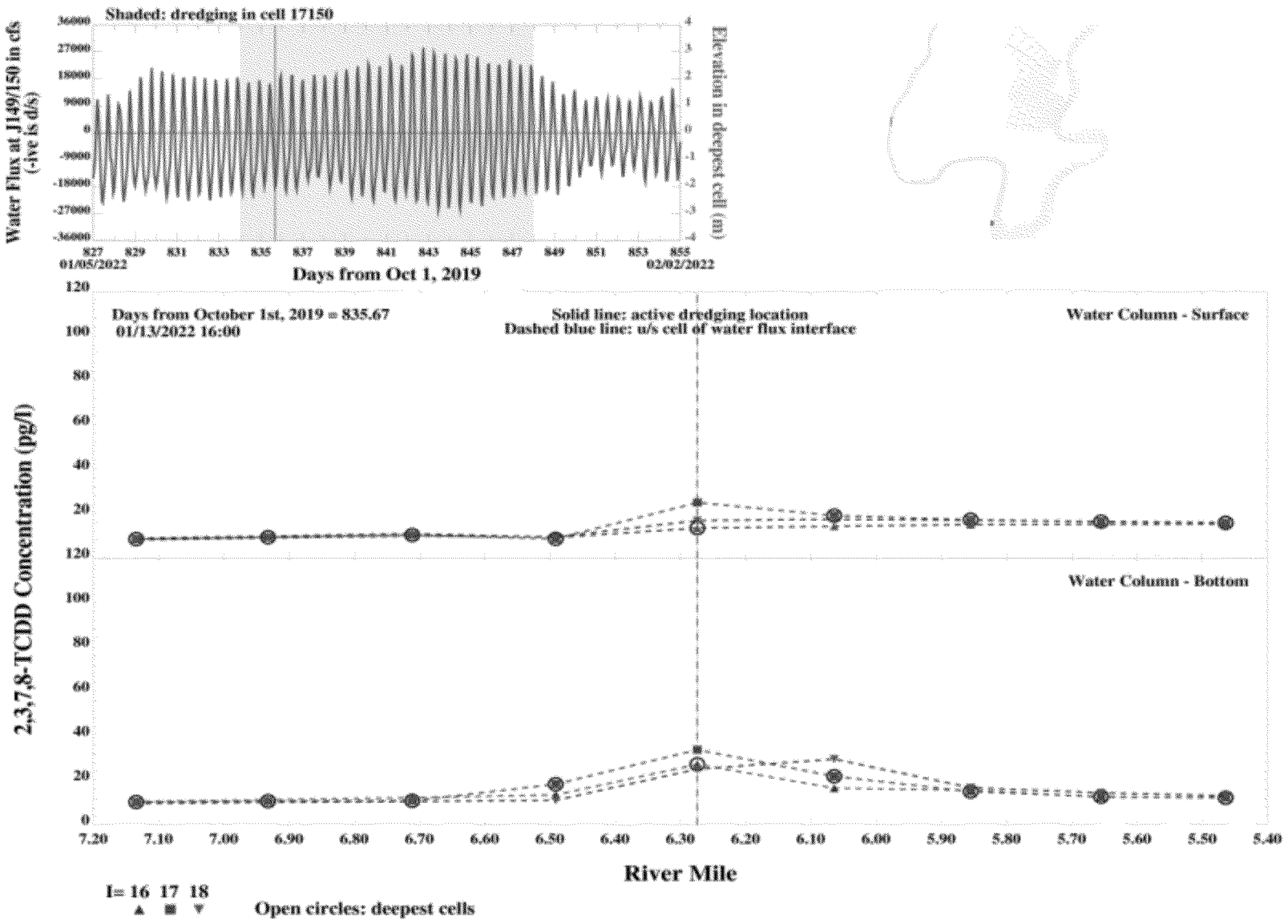

Spatial profile of 2,3,7,8-TCDD water column concentrations during dredging near RM 6.3 - neap tide - peak ebb tide	Figure 12
Lower 8.3 Miles of the Lower Passaic River	2016

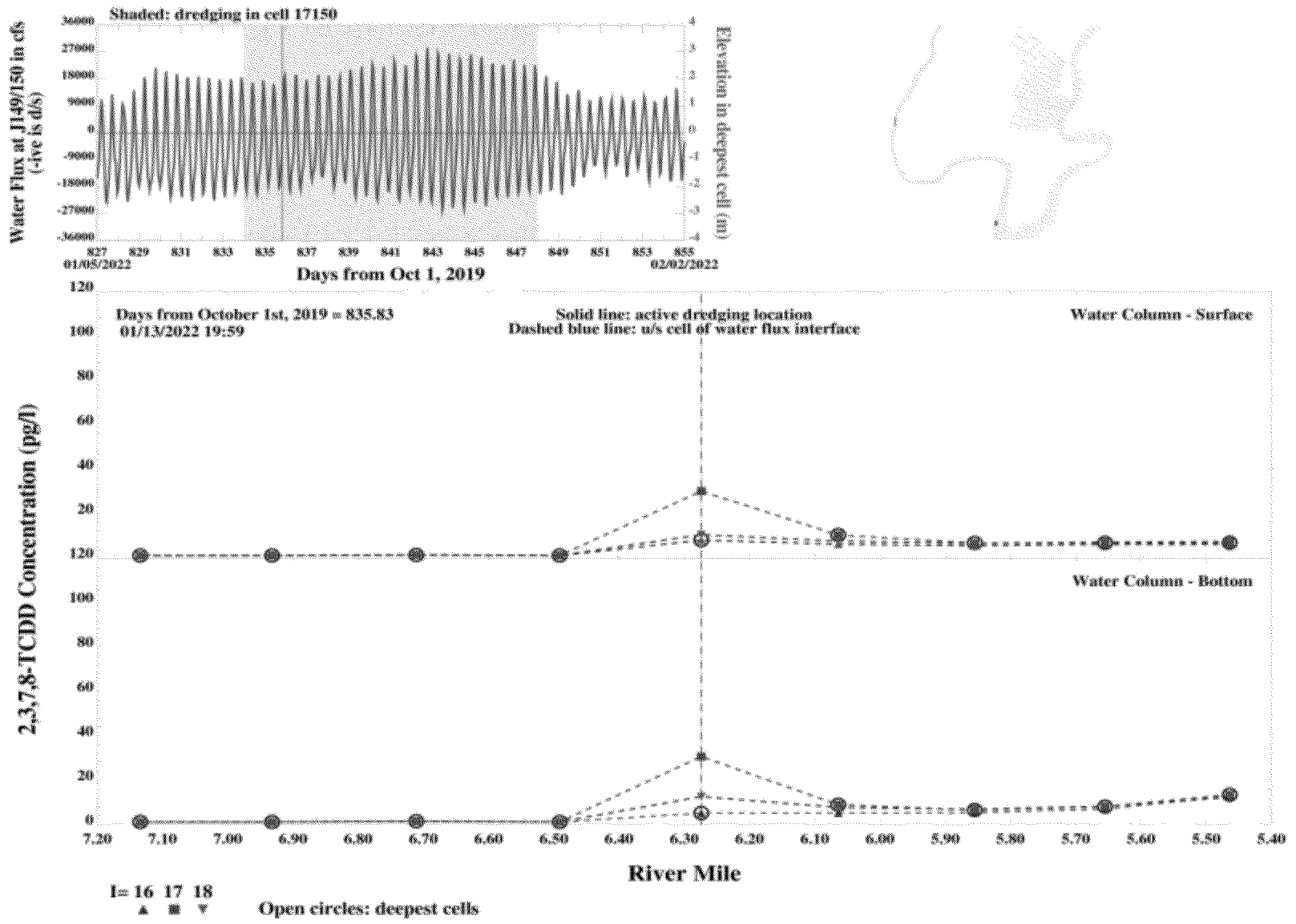

Spatial profile of 2,3,7,8-TCDD water column concentrations during dredging near RM 6.3 - neap tide - low slack tide

Figure 13

Lower 8.3 Miles of the Lower Passaic River

2016

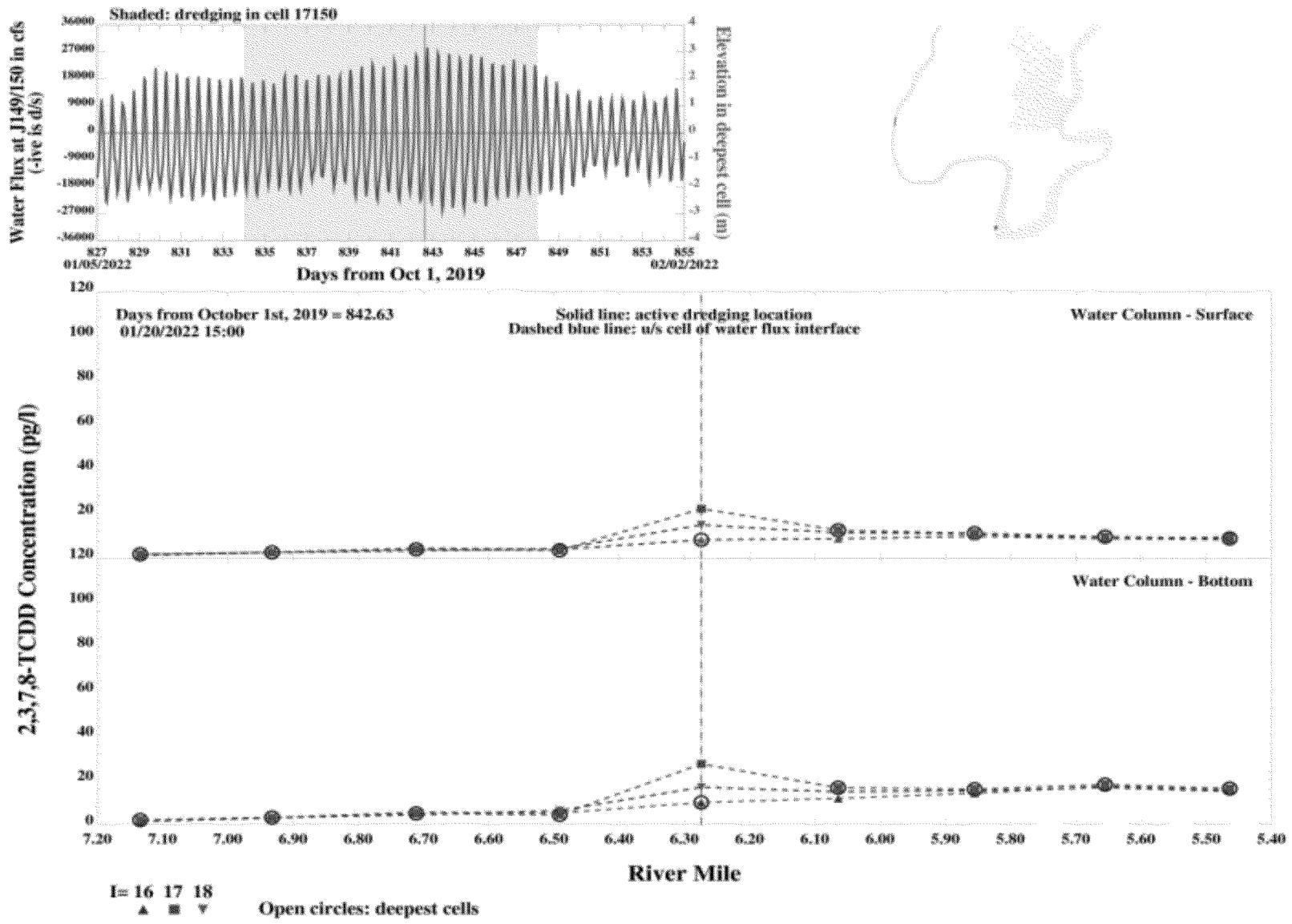

Spatial profile of 2,3,7,8-TCDD water column concentrations during dredging near RM 6.3 - spring tide - low slack tide

Figure 14

Lower 8.3 Miles of the Lower Passaic River

2016

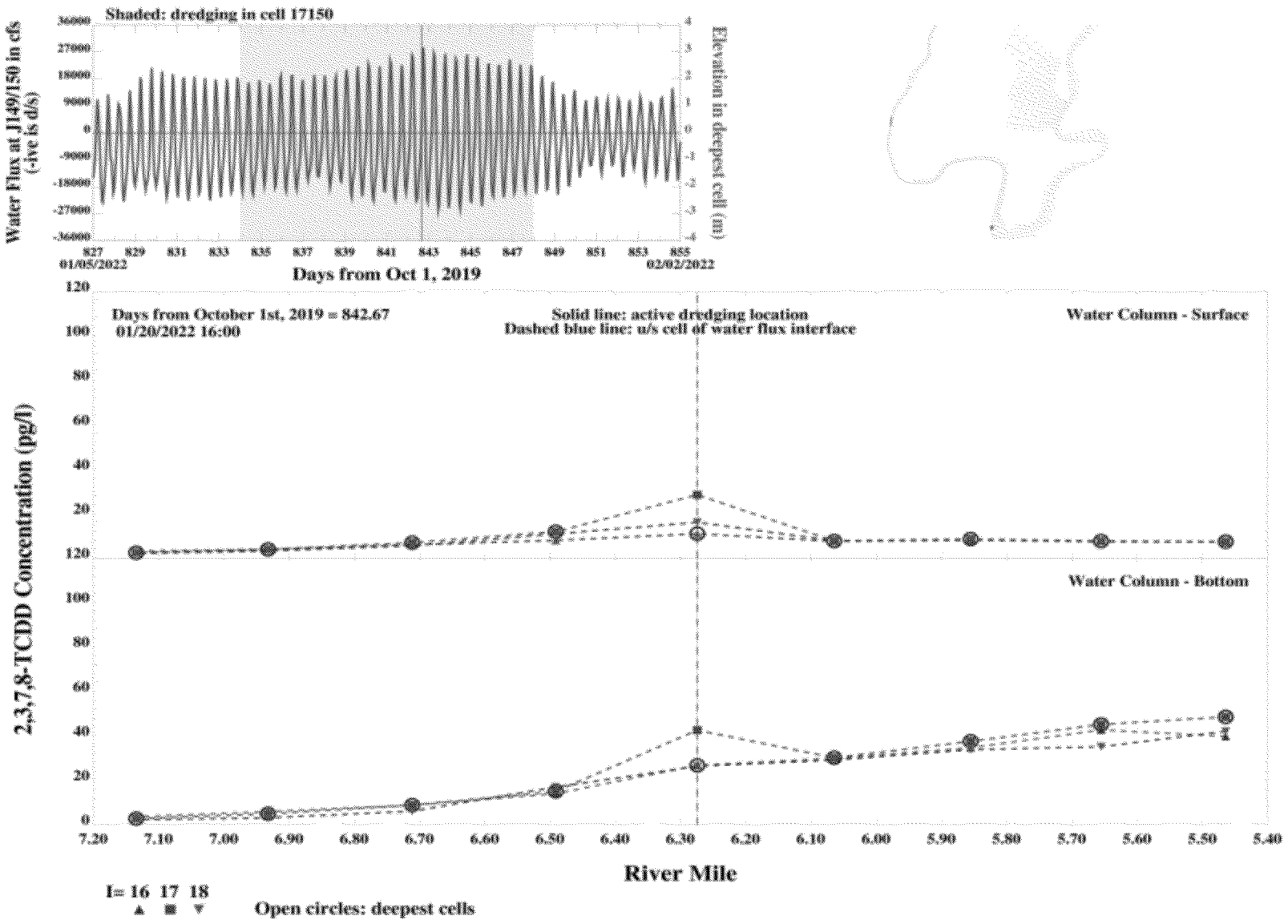

Spatial profile of 2,3,7,8-TCDD water column concentrations during dredging near RM 6.3 - spring tide - flood tide 1 hour after low slack tide

Figure 15

Lower 8.3 Miles of the Lower Passaic River

2016

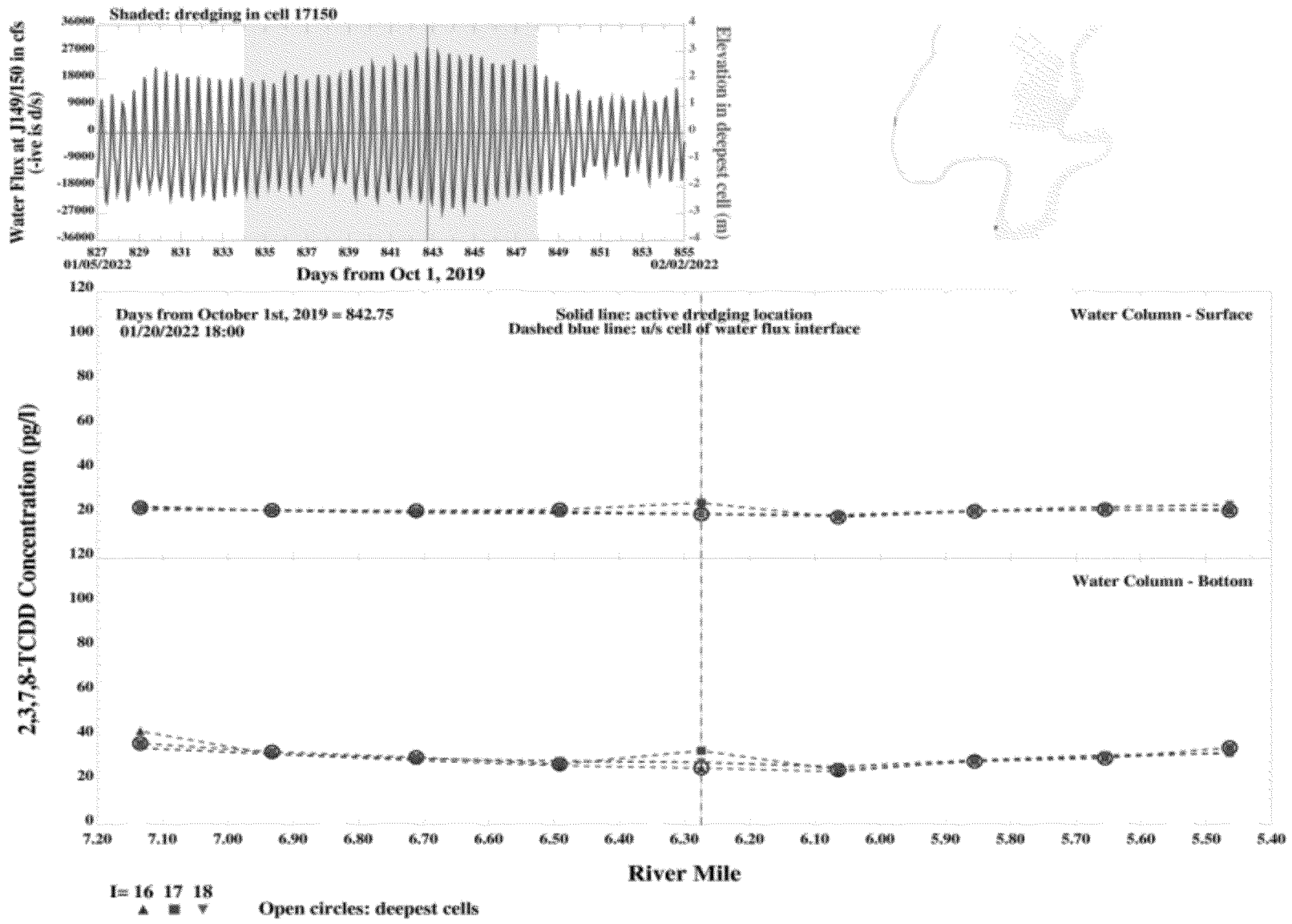

Spatial profile of 2,3,7,8-TCDD water column concentrations during dredging near RM 6.3 - spring tide - peak flood tide

Figure 16

Lower 8.3 Miles of the Lower Passaic River

2016

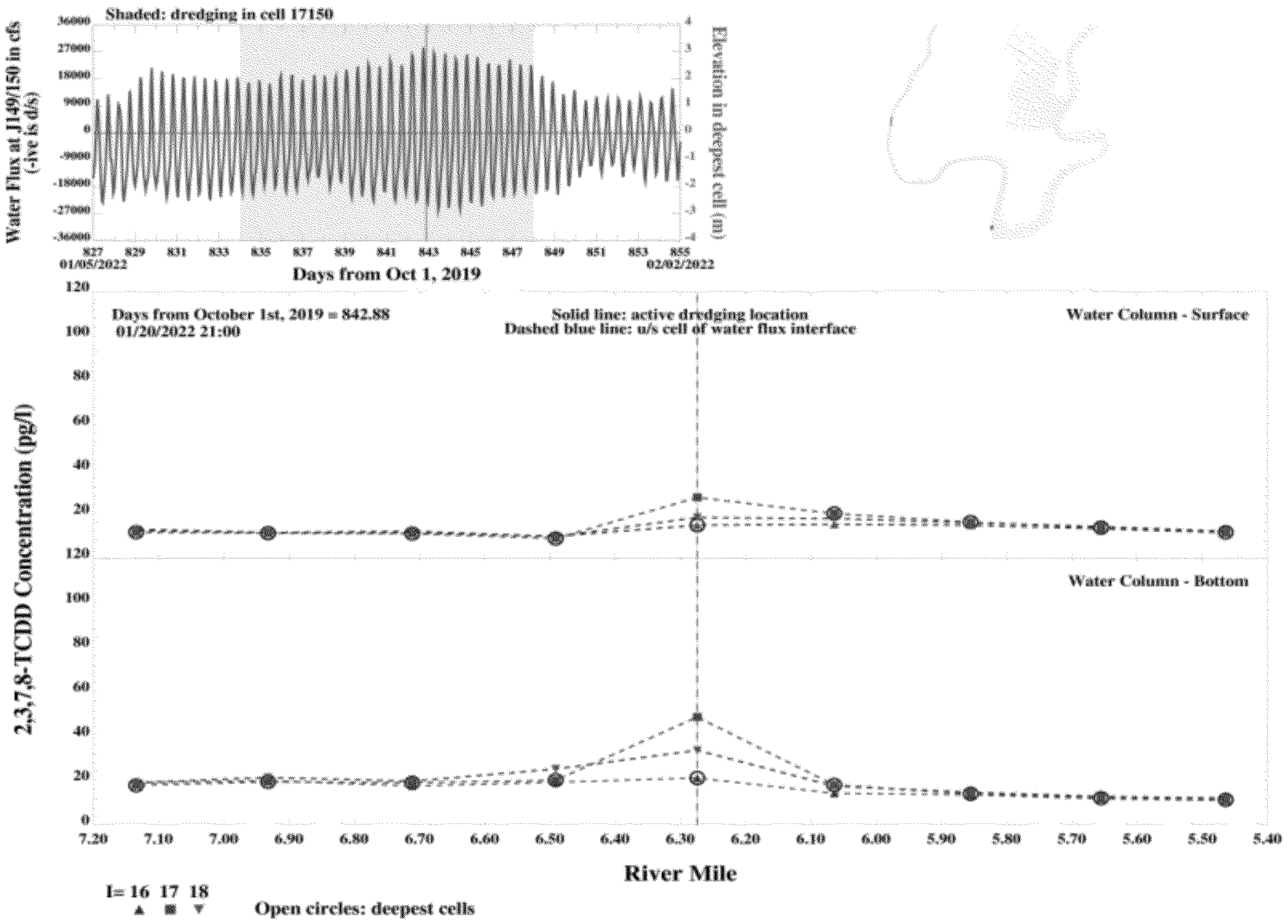

Spatial profile of 2,3,7,8-TCDD water column concentrations during dredging near RM 6.3 - spring tide - high slack tide	Figure 17
Lower 8.3 Miles of the Lower Passaic River	2016

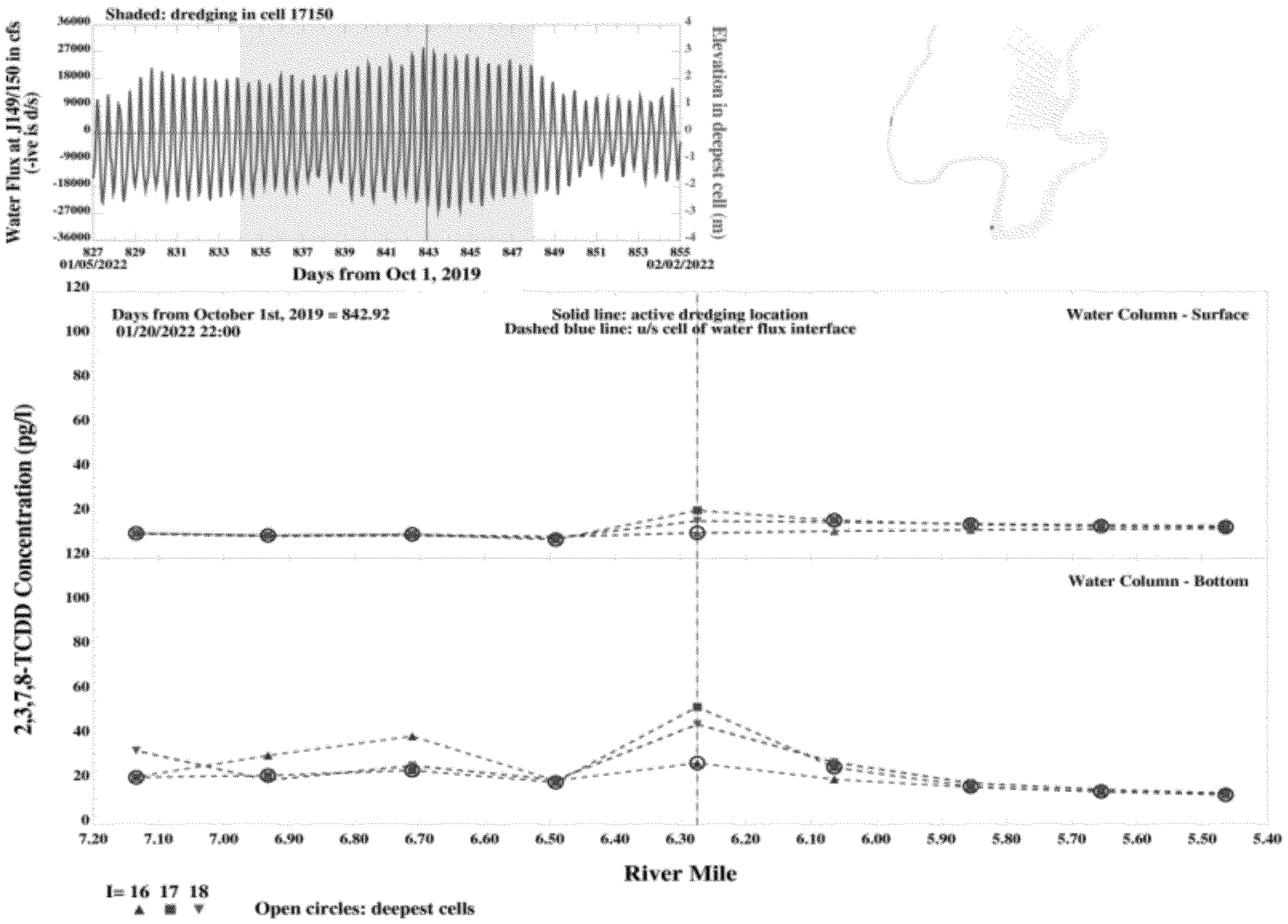

Spatial profile of 2,3,7,8-TCDD water column concentrations during dredging near RM 6.3 - spring tide - ebb tide 1 hour after high slack tide

Figure 18

Lower 8.3 Miles of the Lower Passaic River

2016

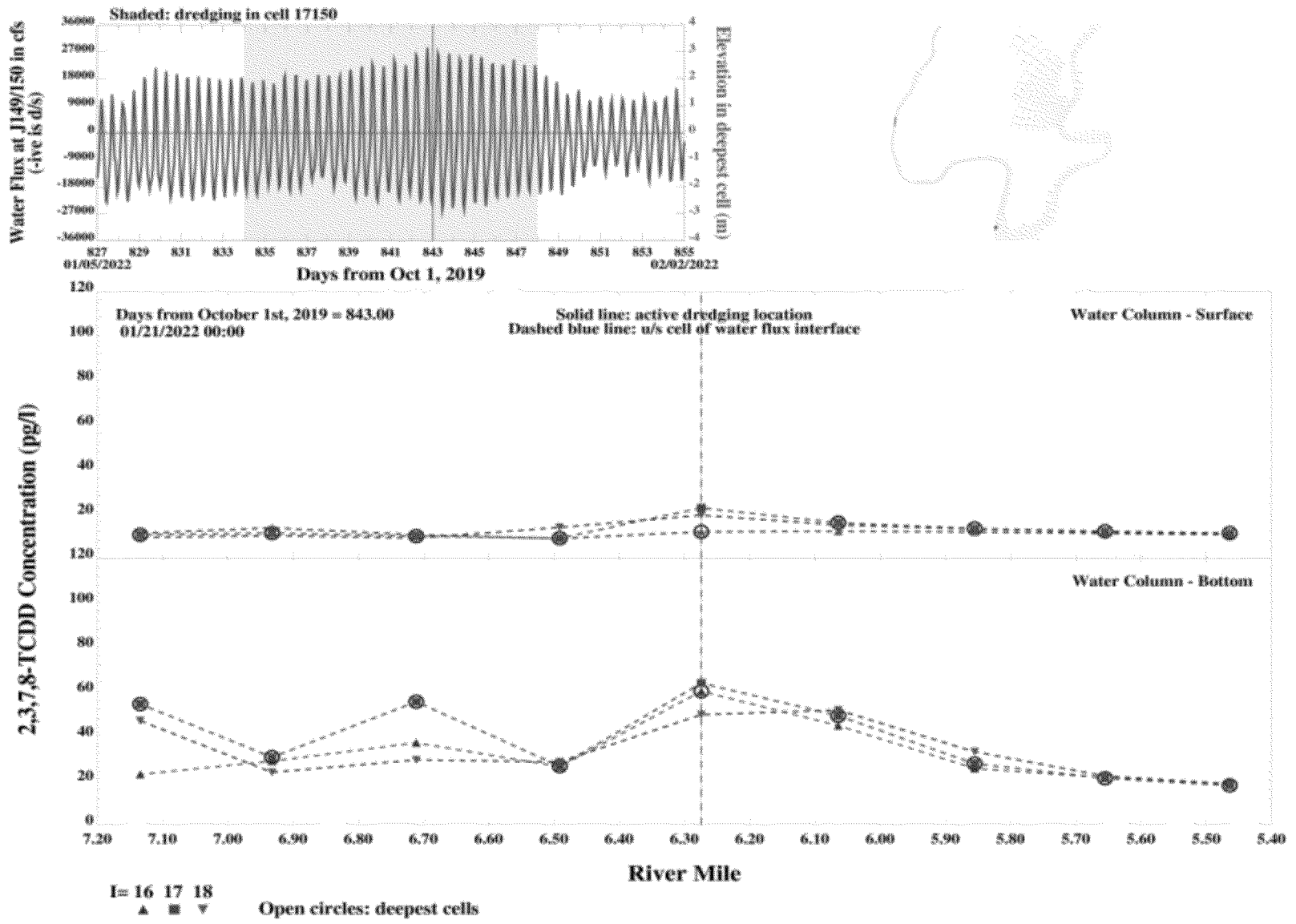

Spatial profile of 2,3,7,8-TCDD water column concentrations during dredging near RM 6.3 - spring tide - peak ebb tide

Figure 19

Lower 8.3 Miles of the Lower Passaic River

2016

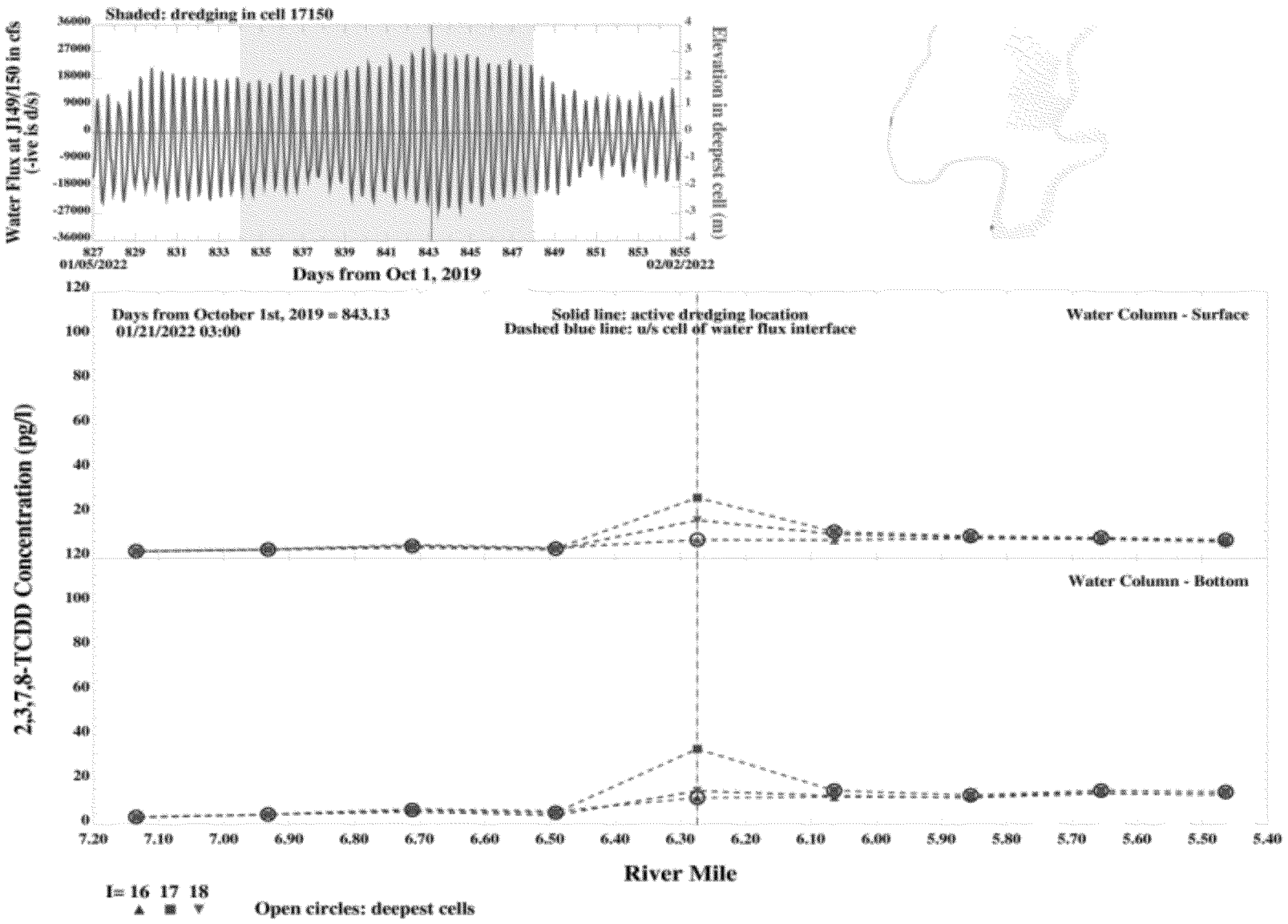

Spatial profile of 2,3,7,8-TCDD water column concentrations during dredging near RM 6.3 - spring tide - low slack tide	Figure 20
Lower 8.3 Miles of the Lower Passaic River	2016

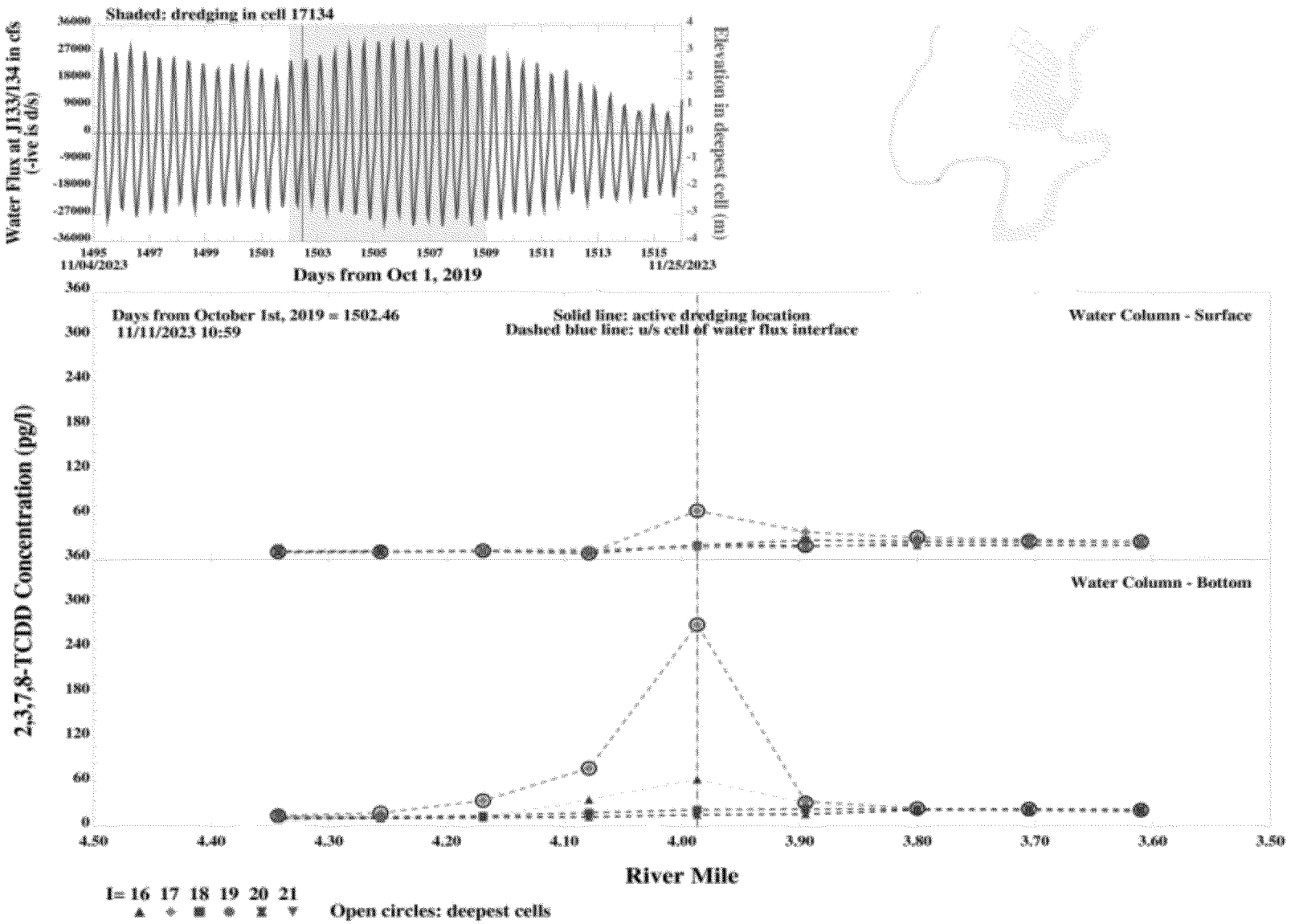

Spatial profile of 2,3,7,8-TCDD water column concentrations during dredging near RM 4 - neap tide - low slack tide	Figure 21
Lower 8.3 Miles of the Lower Passaic River	2016

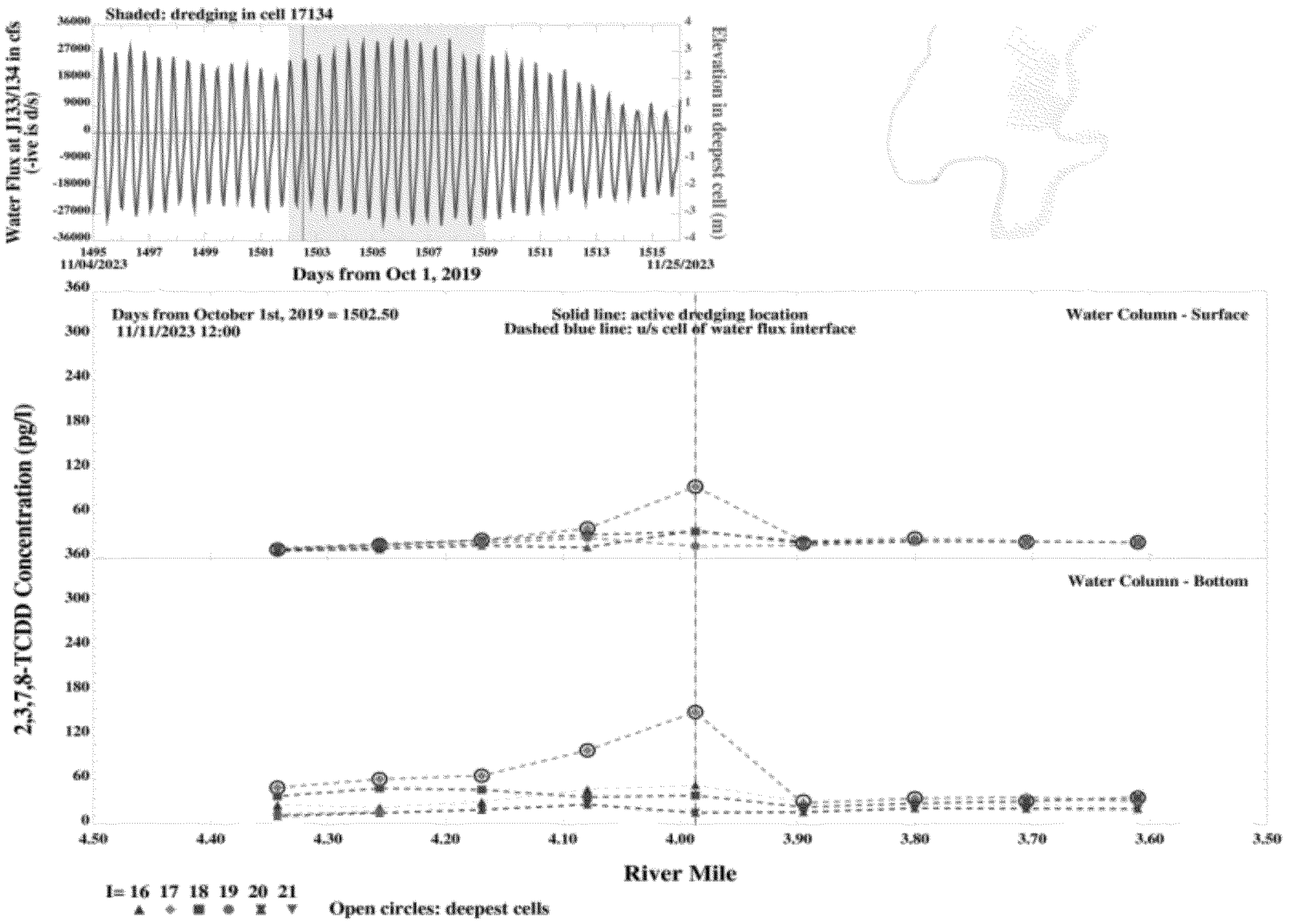

Spatial profile of 2,3,7,8-TCDD water column concentrations during dredging near RM 4 - neap tide - flood tide 1 hour after low slack tide	Figure 22
Lower 8.3 Miles of the Lower Passaic River	2016

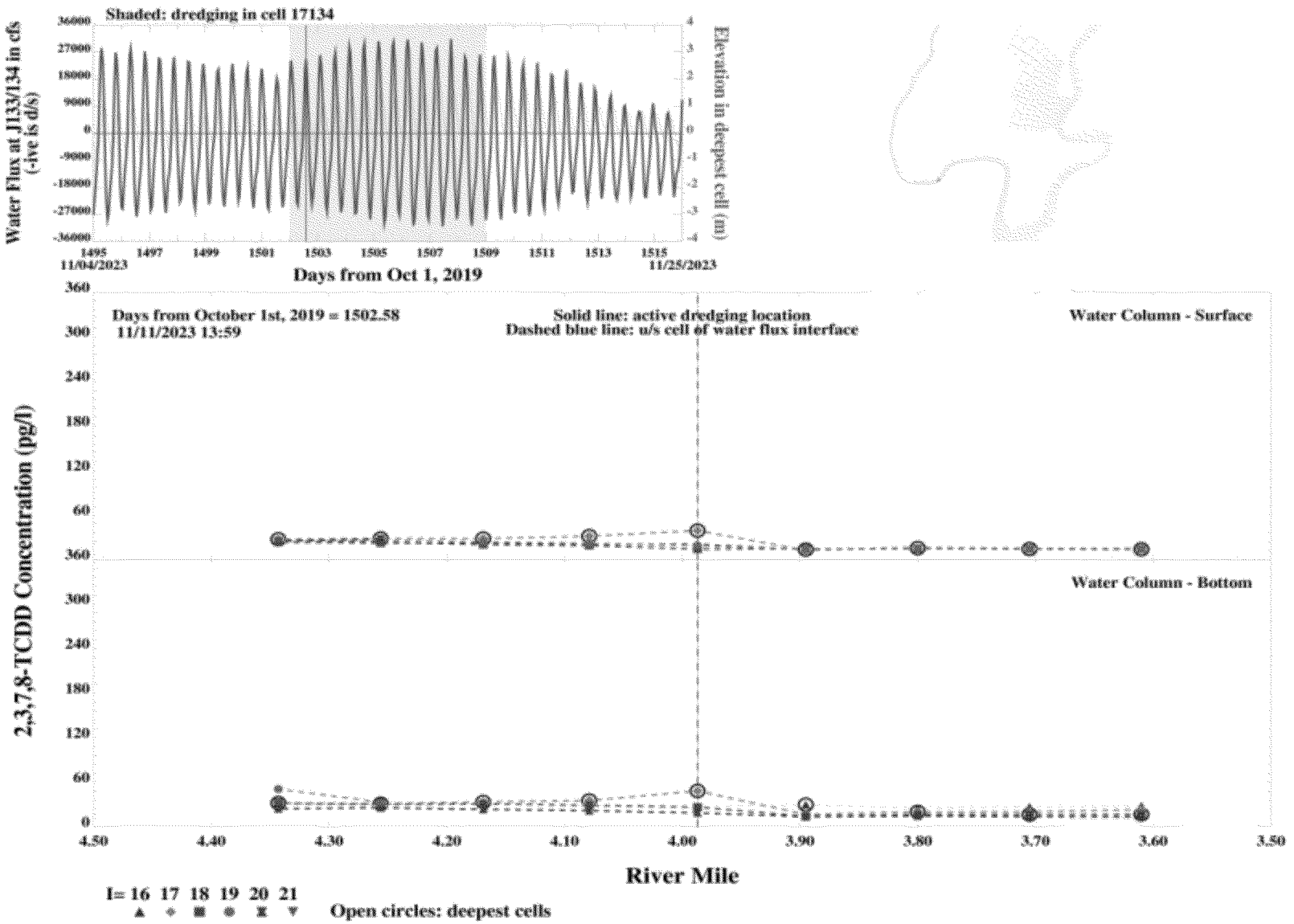

Spatial profile of 2,3,7,8-TCDD water column concentrations during dredging near RM 4 - neap tide - peak flood tide

Figure 23

Lower 8.3 Miles of the Lower Passaic River

2016

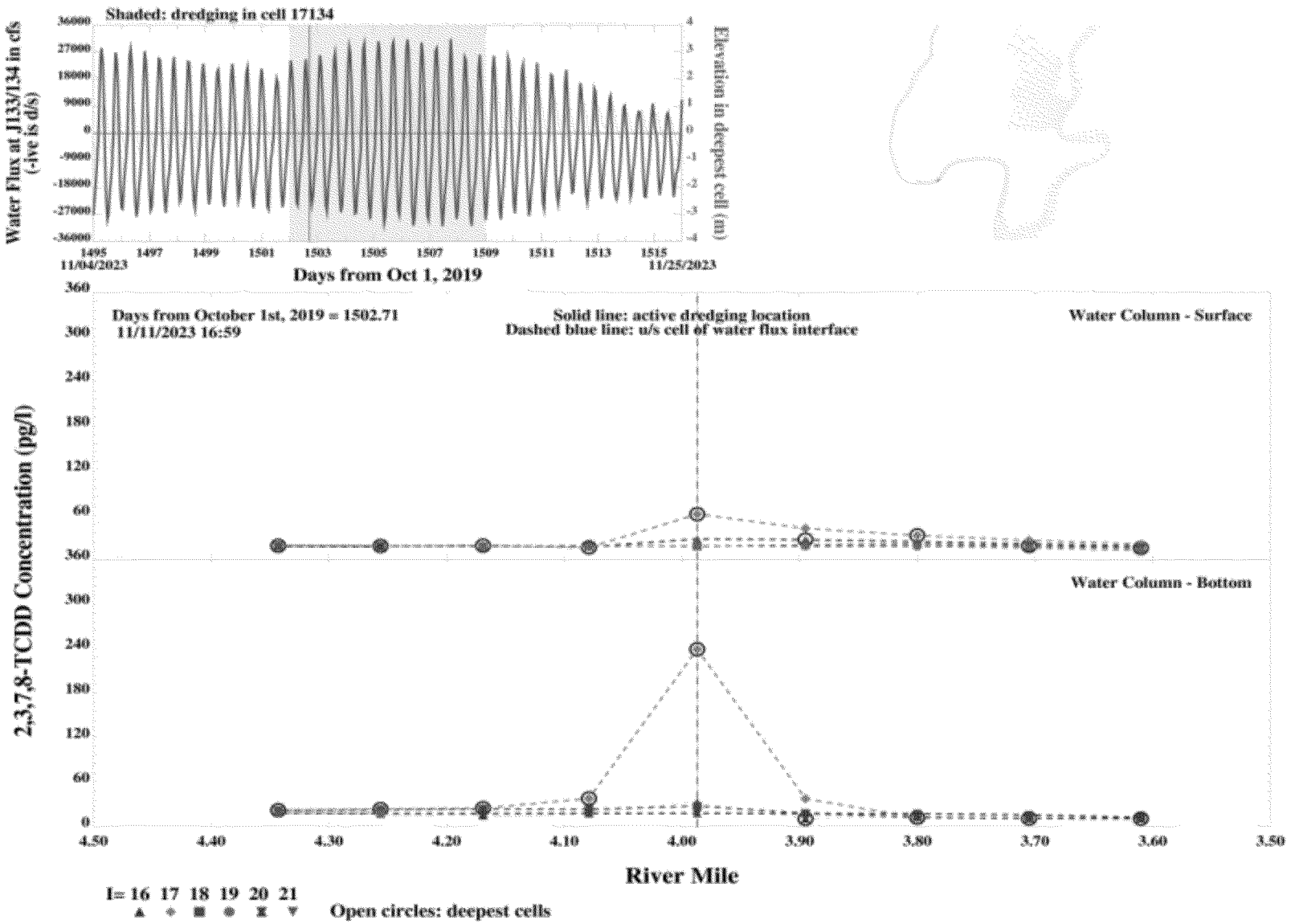

Spatial profile of 2,3,7,8-TCDD water column concentrations during dredging near RM 4 - neap tide - high slack tide	Figure 24
Lower 8.3 Miles of the Lower Passaic River	2016

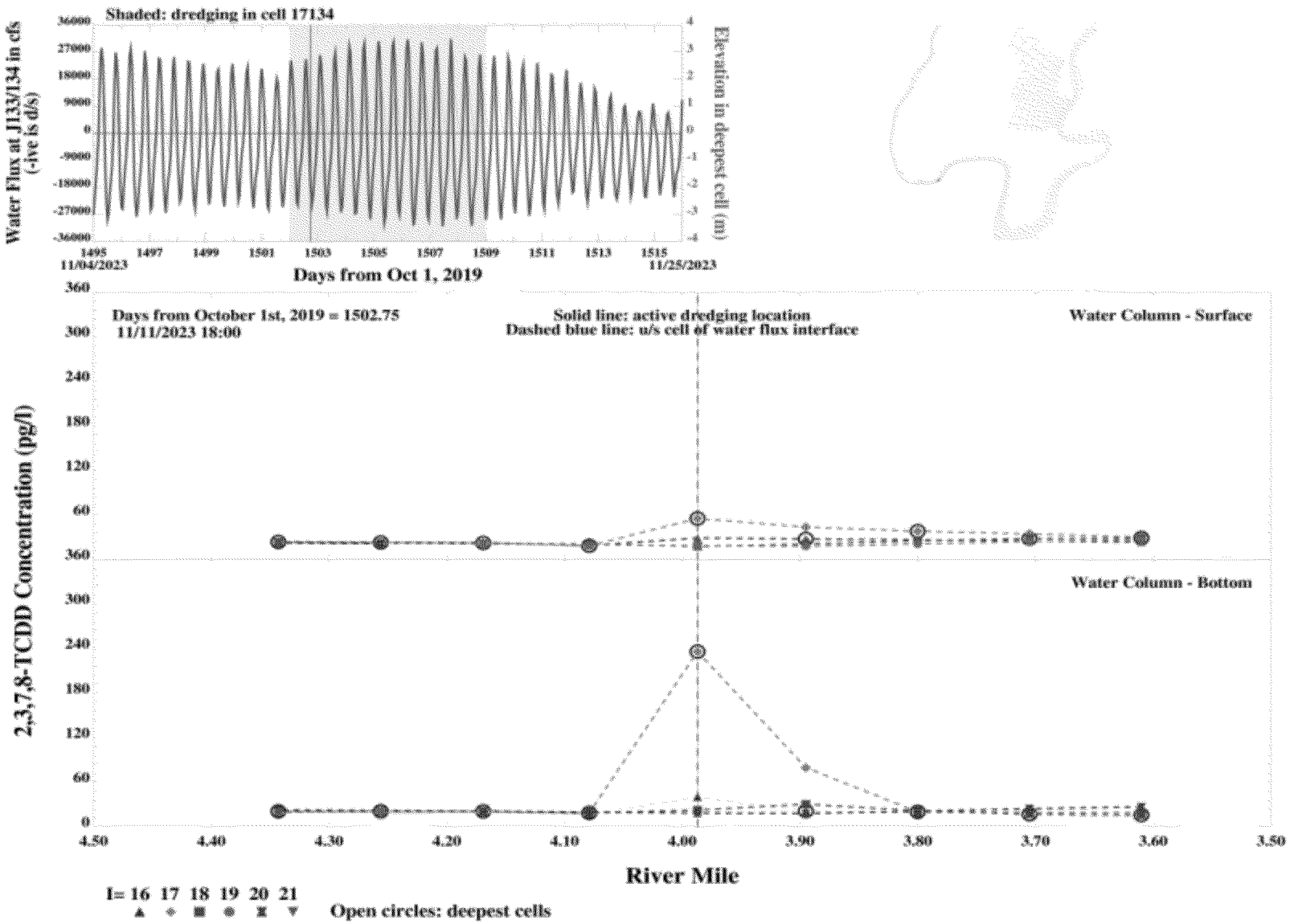

Spatial profile of 2,3,7,8-TCDD water column concentrations during dredging near RM 4 - neap tide - ebb tide 1 hour after high slack tide	Figure 25
Lower 8.3 Miles of the Lower Passaic River	2016

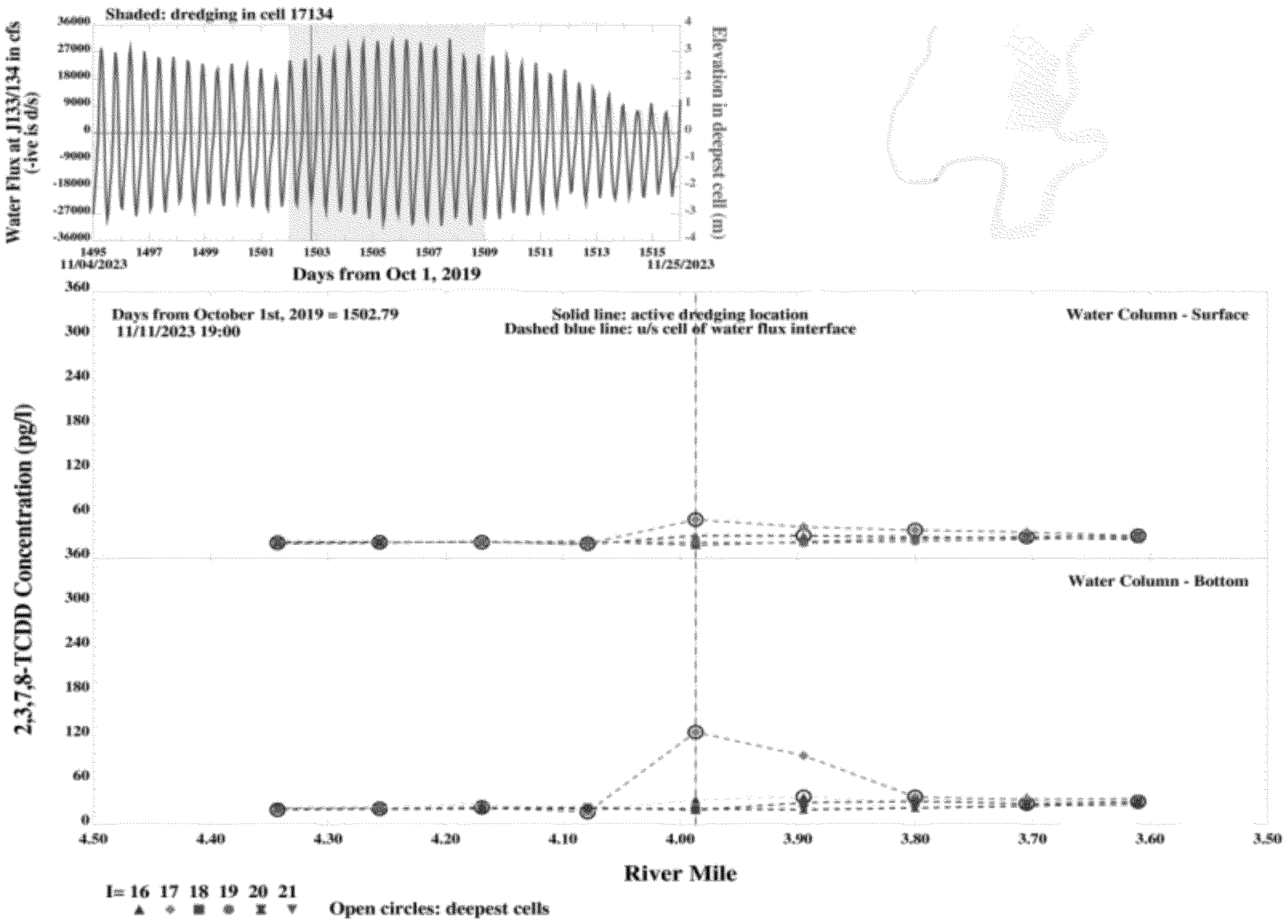

Spatial profile of 2,3,7,8-TCDD water column concentrations during dredging near RM 4 - neap tide - peak ebb tide

Figure 26

Lower 8.3 Miles of the Lower Passaic River

2016

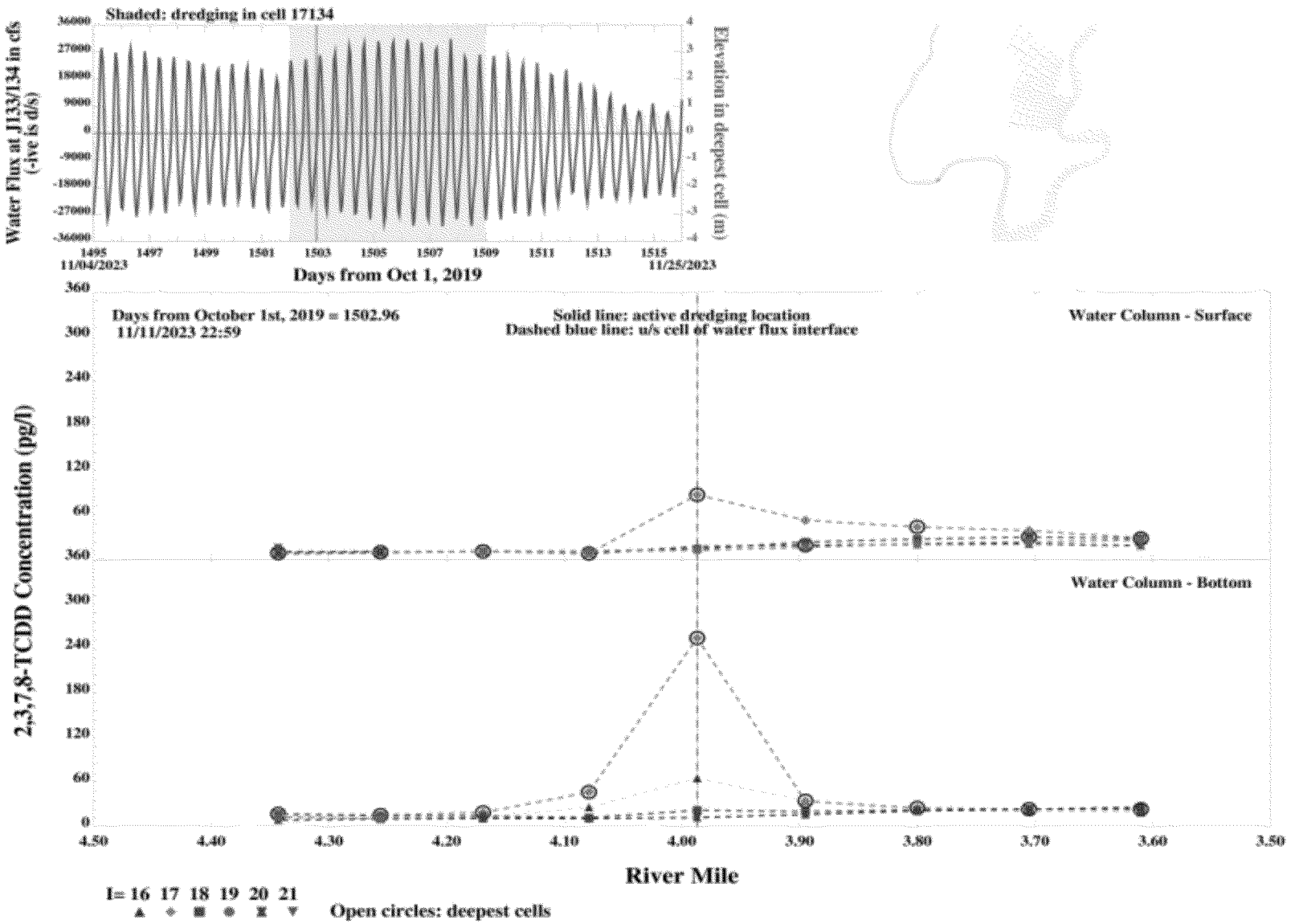

Spatial profile of 2,3,7,8-TCDD water column concentrations during dredging near RM 4 - neap tide - low slack tide	Figure 27
Lower 8.3 Miles of the Lower Passaic River	2016

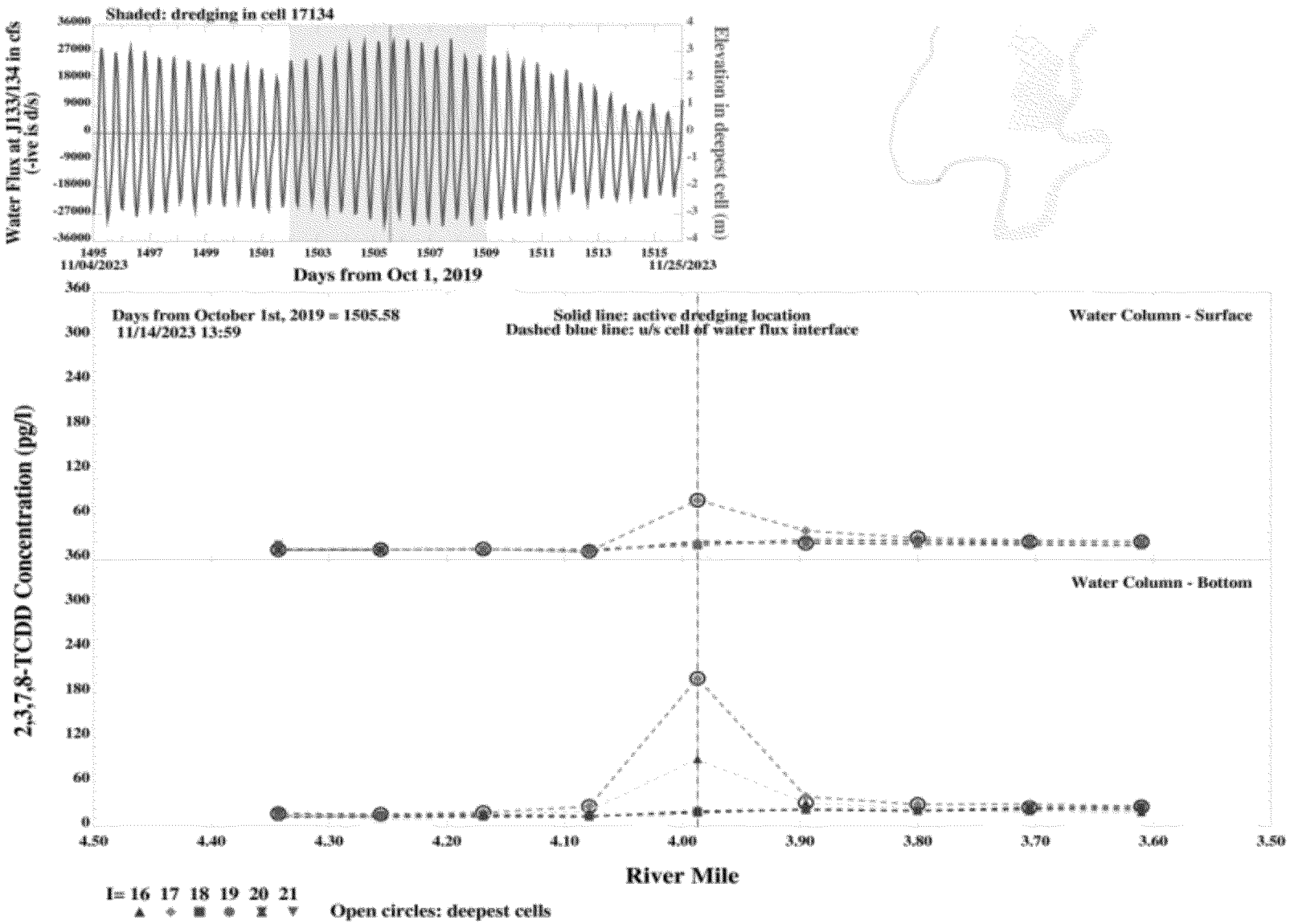

Spatial profile of 2,3,7,8-TCDD water column concentrations during dredging near RM 4 - spring tide - low slack tide	Figure 28
Lower 8.3 Miles of the Lower Passaic River	2016

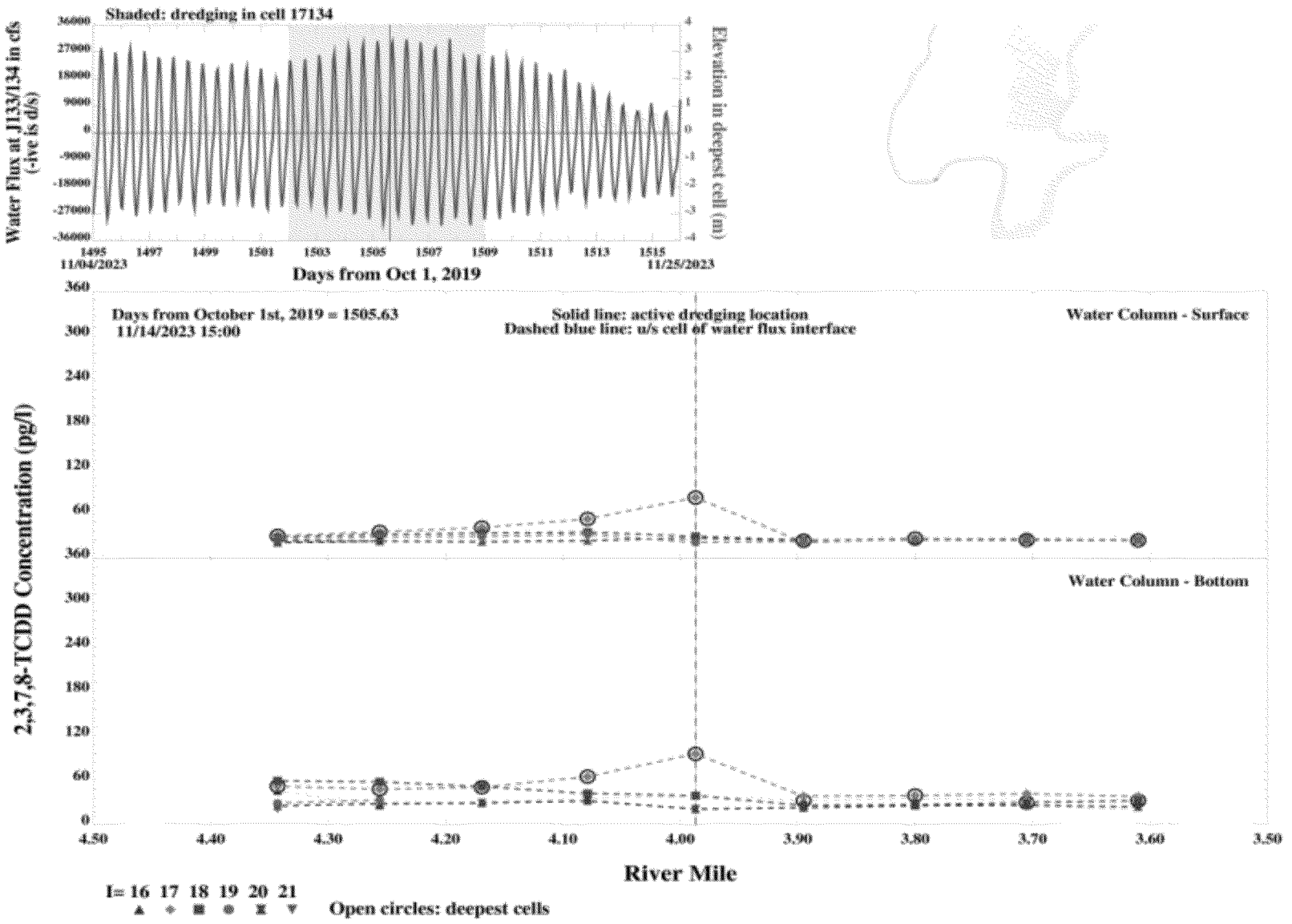

Spatial profile of 2,3,7,8-TCDD water column concentrations during dredging near RM 4 - spring tide - flood tide 1 hour after low slack tide	Figure 29
Lower 8.3 Miles of the Lower Passaic River	2016

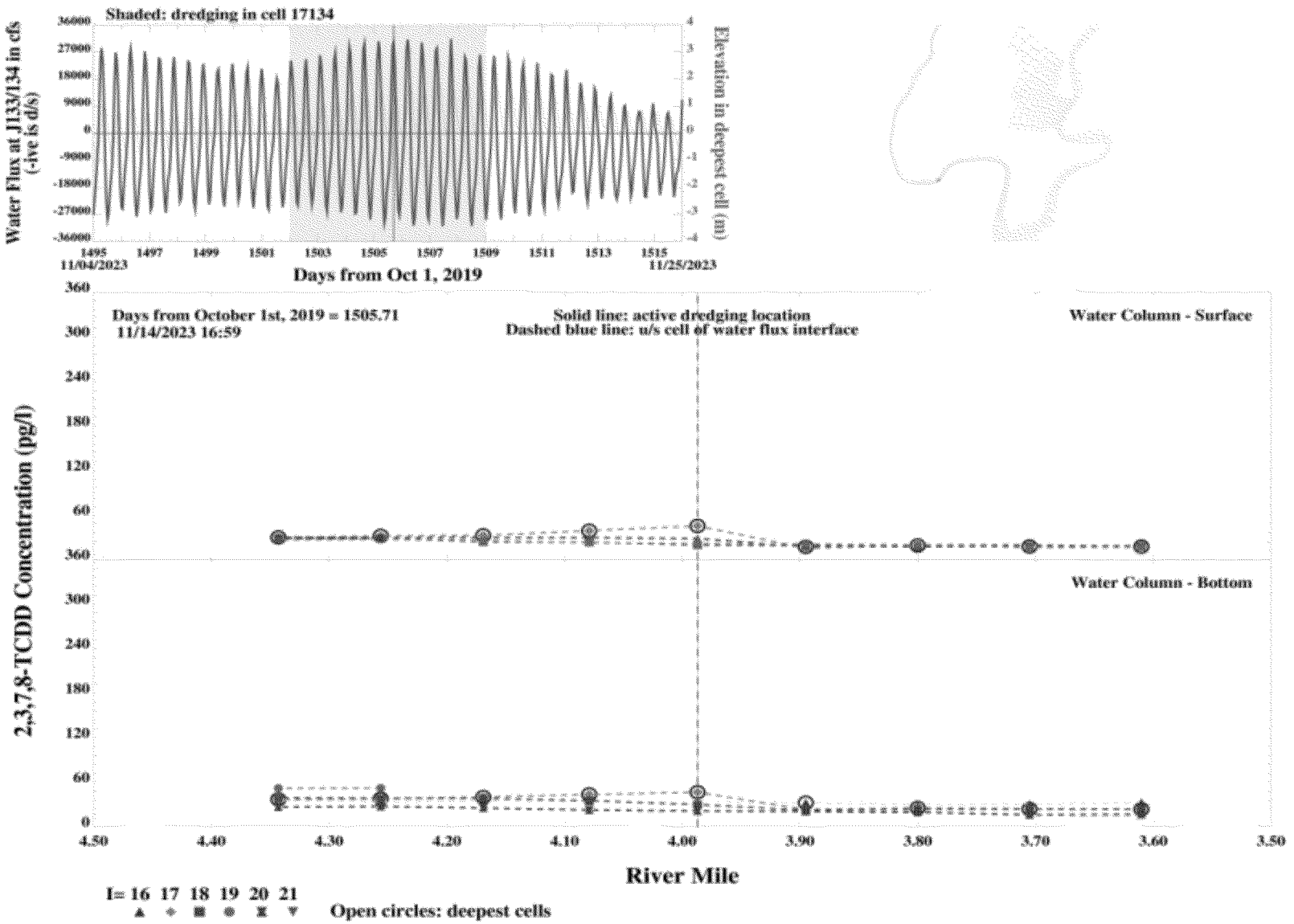

Spatial profile of 2,3,7,8-TCDD water column concentrations during dredging near RM 4 - spring tide - peak flood tide	Figure 30
Lower 8.3 Miles of the Lower Passaic River	2016

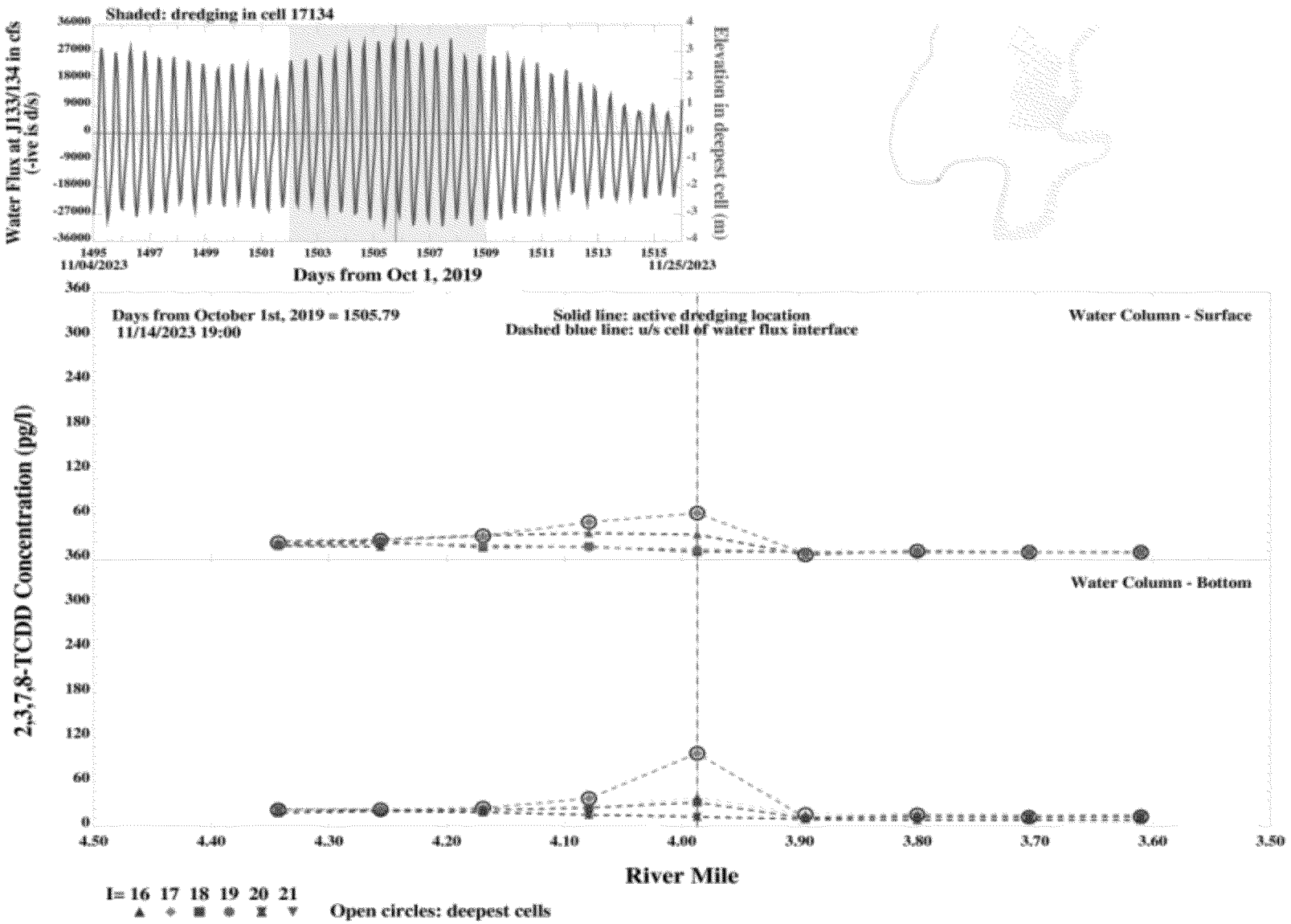

Spatial profile of 2,3,7,8-TCDD water column concentrations during dredging near RM 4 - spring tide - high slack tide	Figure 31
Lower 8.3 Miles of the Lower Passaic River	2016

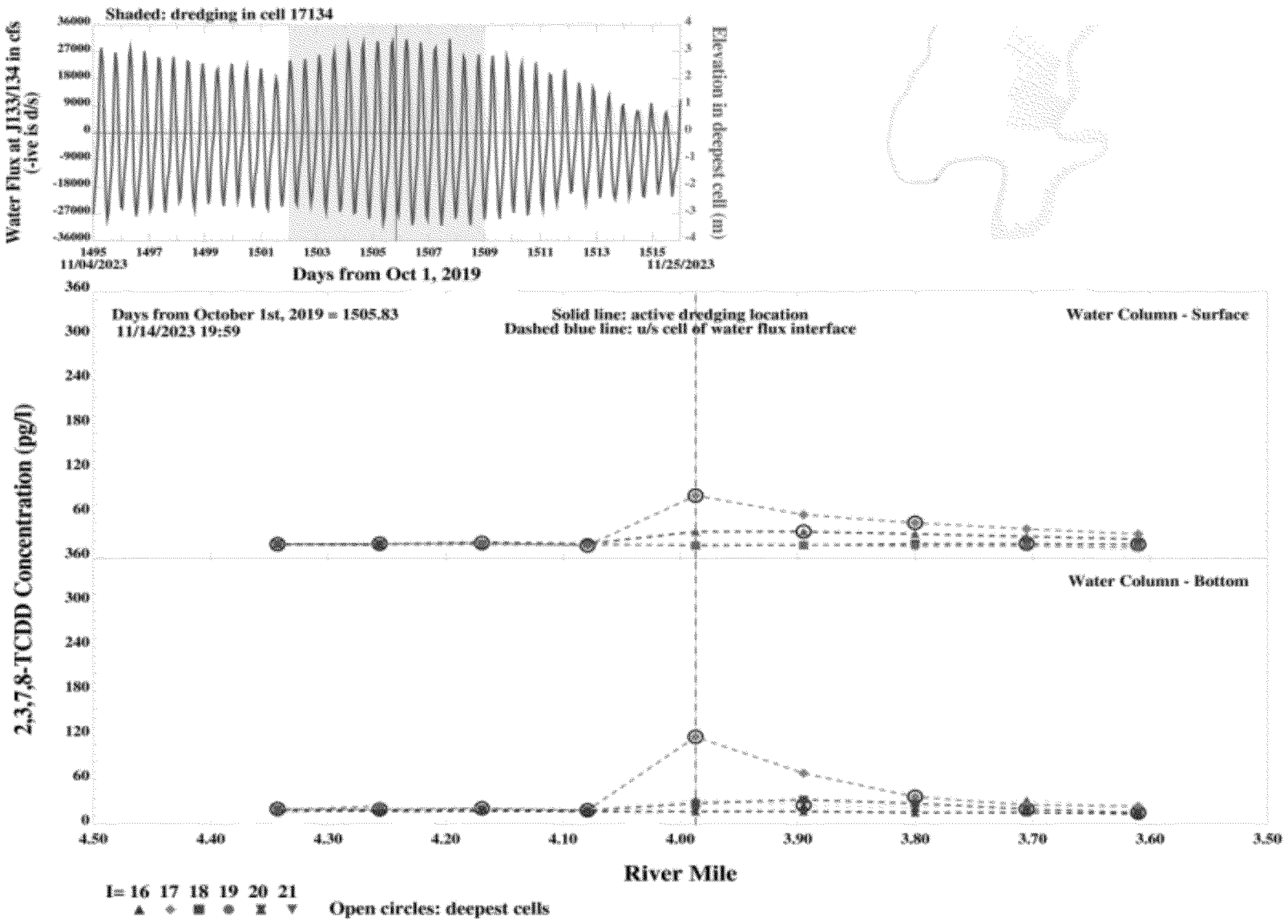

Spatial profile of 2,3,7,8-TCDD water column concentrations during dredging near RM 4 - spring tide - ebb tide 1 hour after high slack tide	Figure 32
Lower 8.3 Miles of the Lower Passaic River	2016

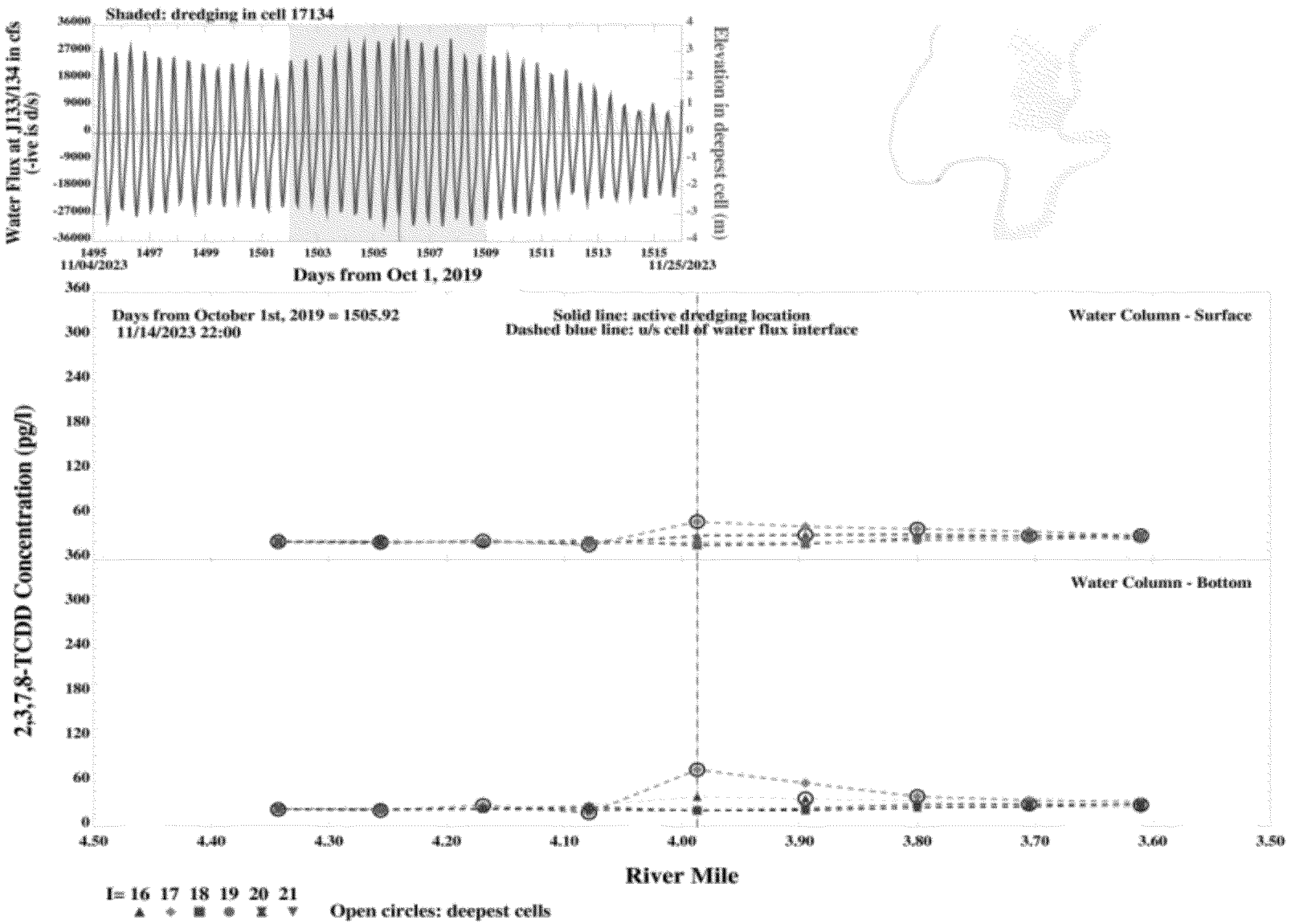

Spatial profile of 2,3,7,8-TCDD water column concentrations during dredging near RM 4 - spring tide - peak ebb tide	Figure 33
Lower 8.3 Miles of the Lower Passaic River	2016

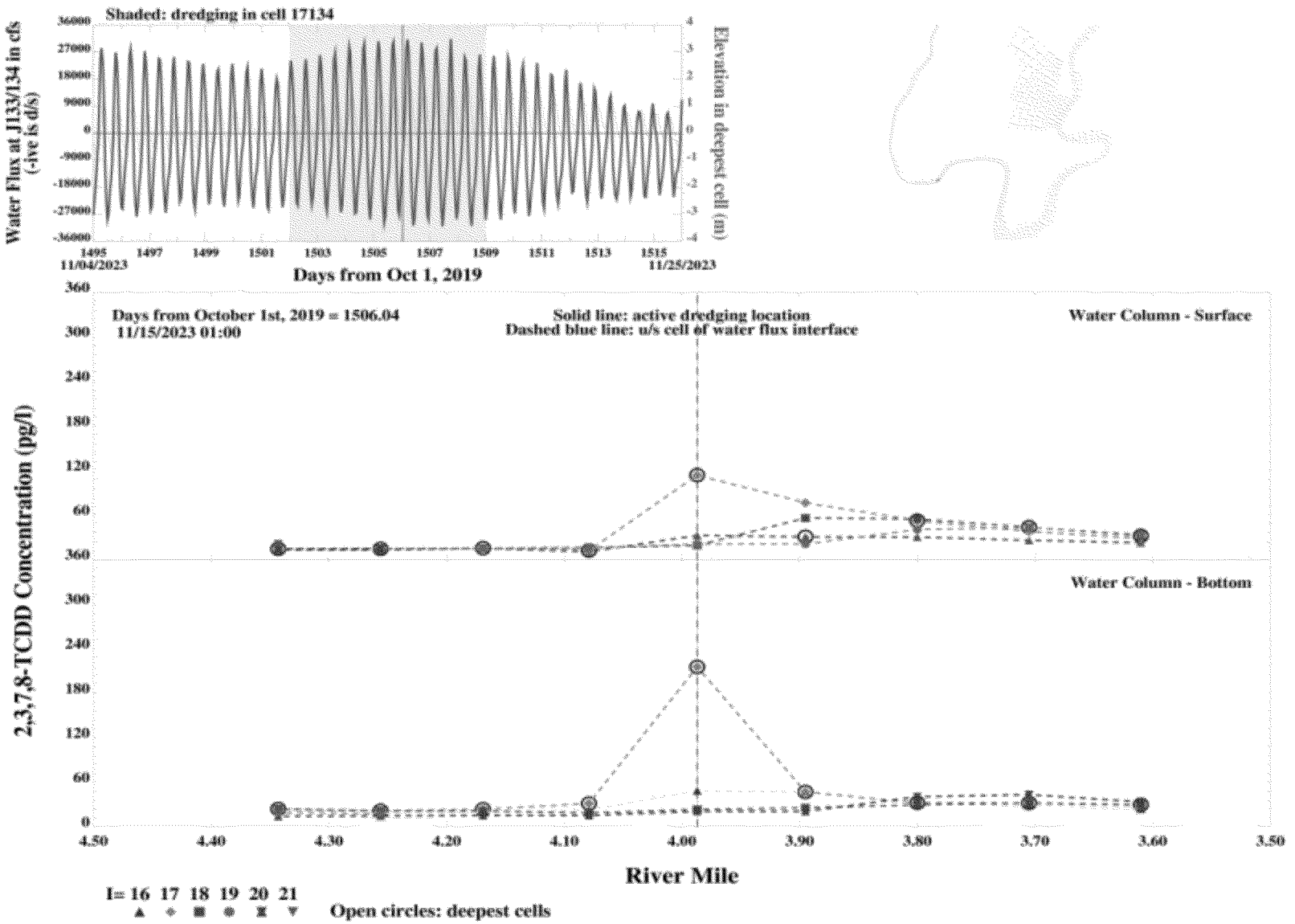

Spatial profile of 2,3,7,8-TCDD water column concentrations during dredging near RM 4 - spring tide - low slack tide	Figure 34
Lower 8.3 Miles of the Lower Passaic River	2016

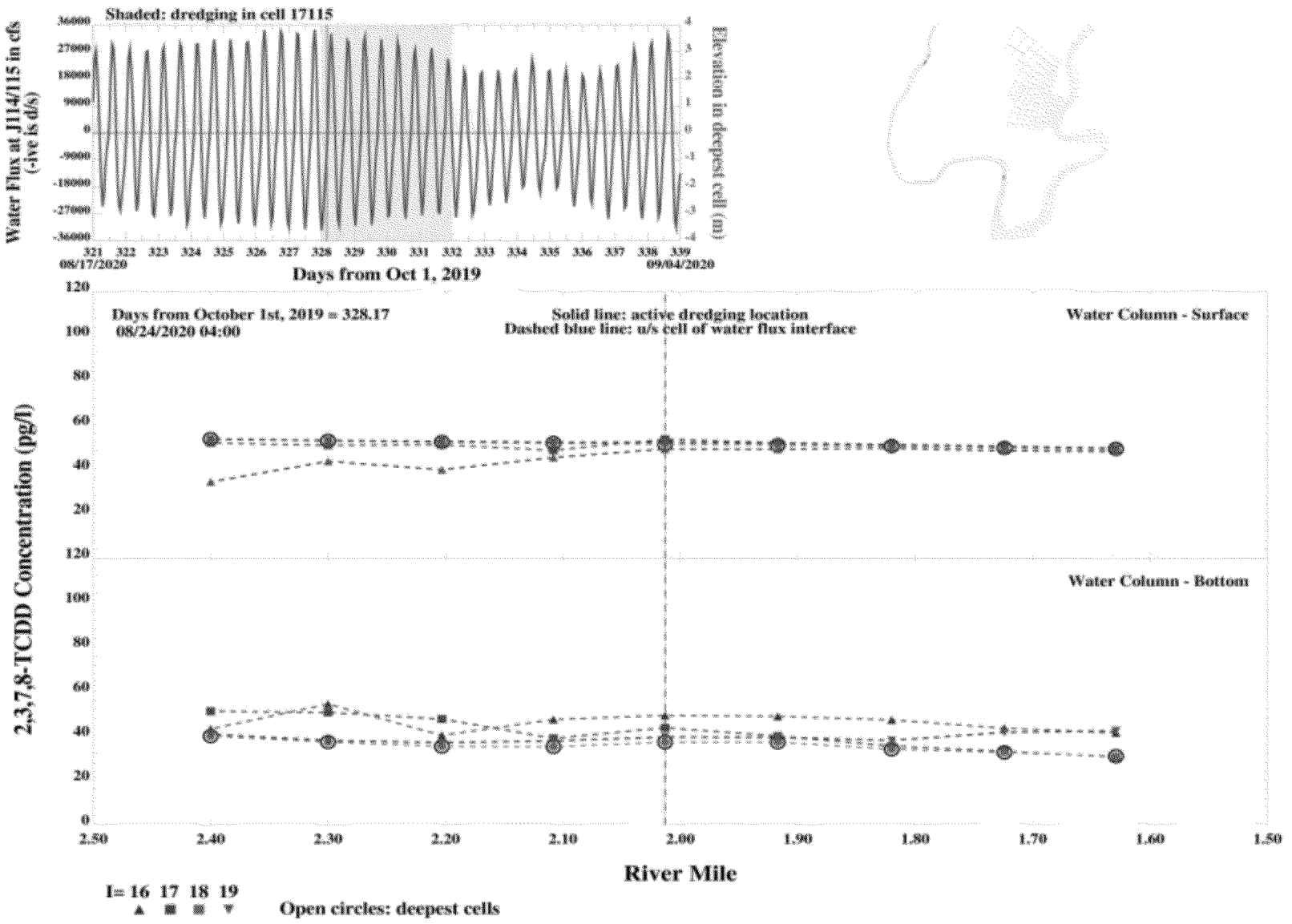

Spatial profile of 2,3,7,8-TCDD water column concentrations during dredging near RM 2 - spring tide - low slack tide

Figure 35

Lower 8.3 Miles of the Lower Passaic River

2016

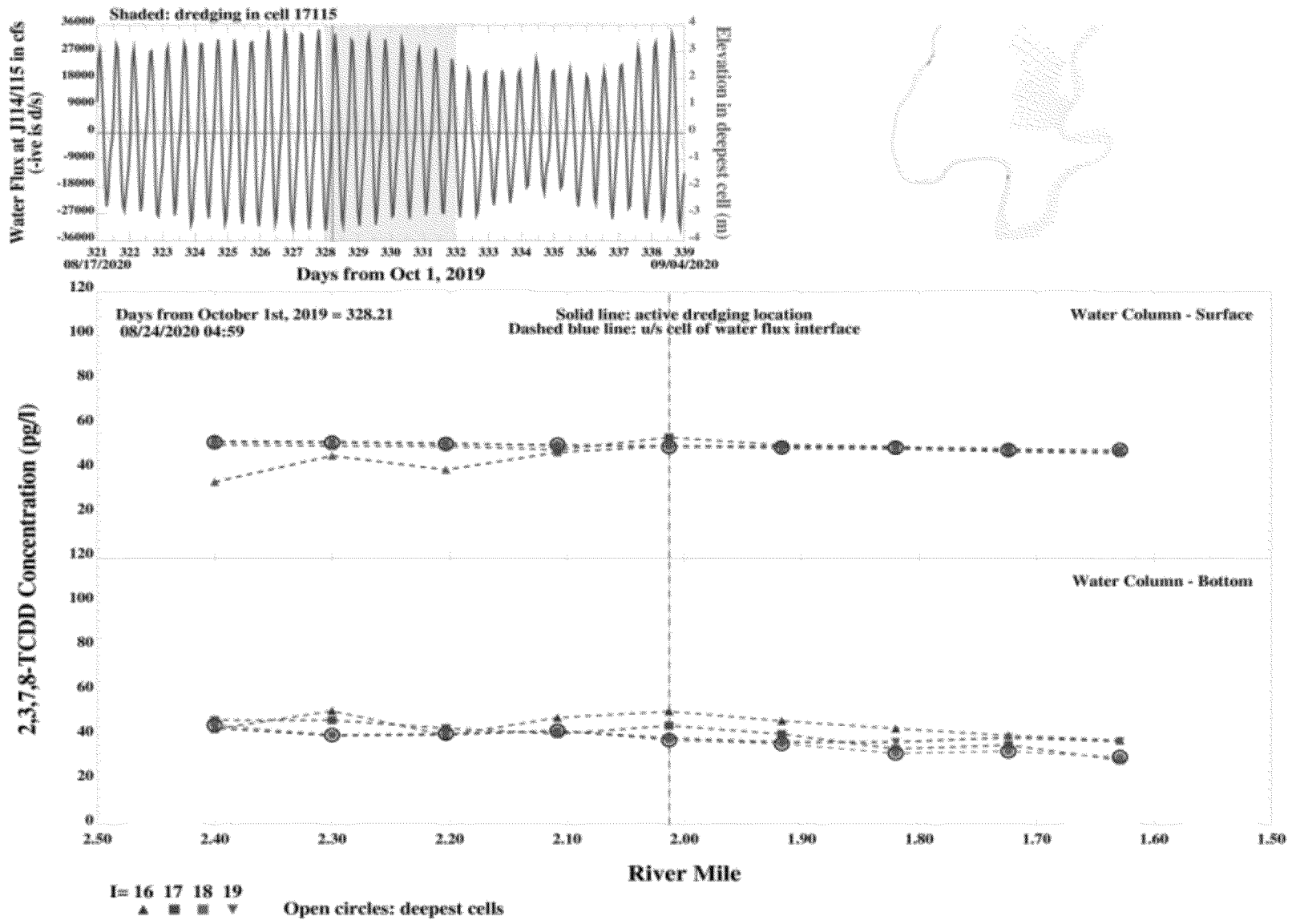

Spatial profile of 2,3,7,8-TCDD water column concentrations during dredging near RM 2 - spring tide - flood tide 1 hour after low slack tide

Lower 8.3 Miles of the Lower Passaic River

Figure 36

2016

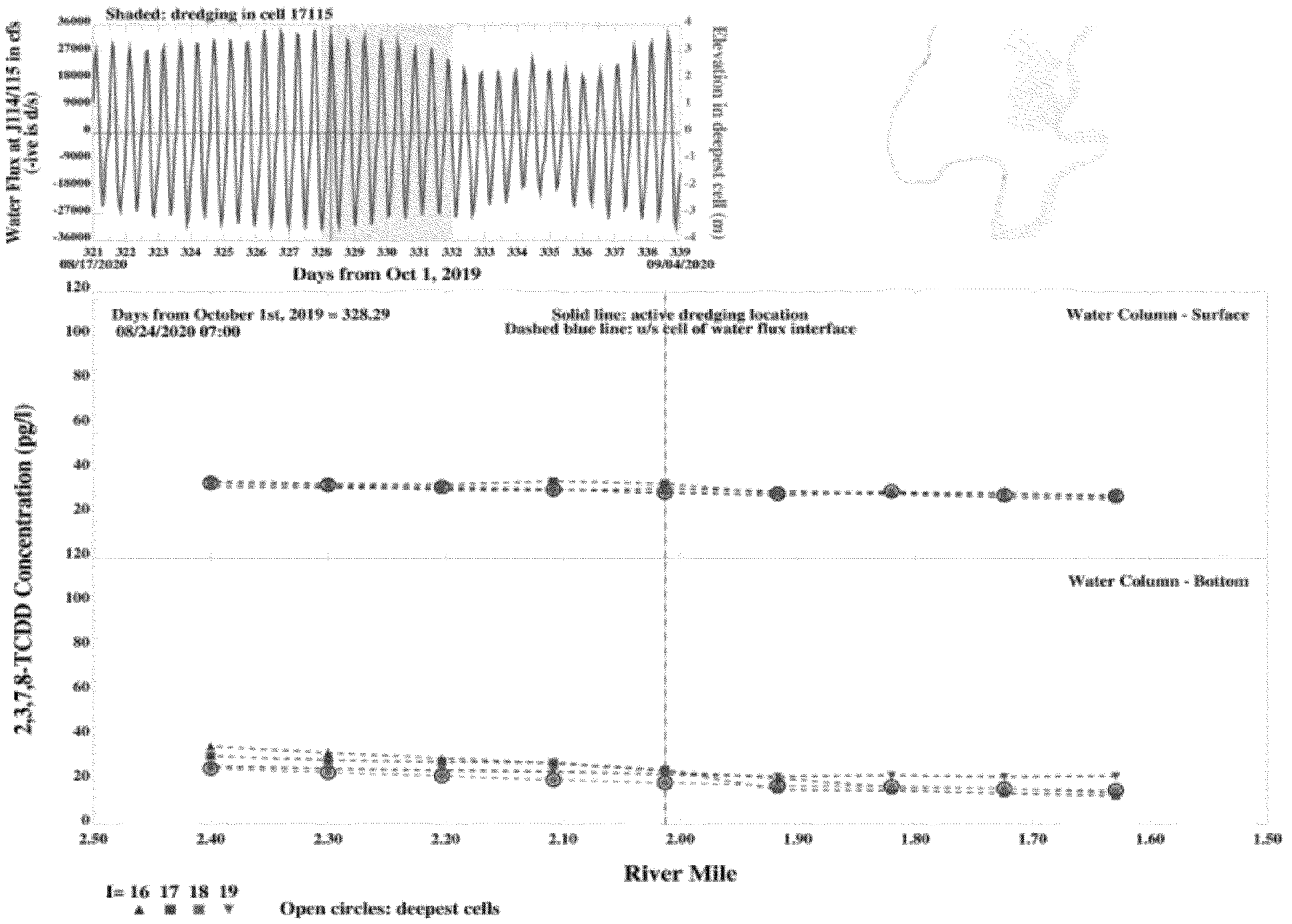

Spatial profile of 2,3,7,8-TCDD water column concentrations during dredging near RM 2 - spring tide - peak flood tide

Figure 37

Lower 8.3 Miles of the Lower Passaic River

2016

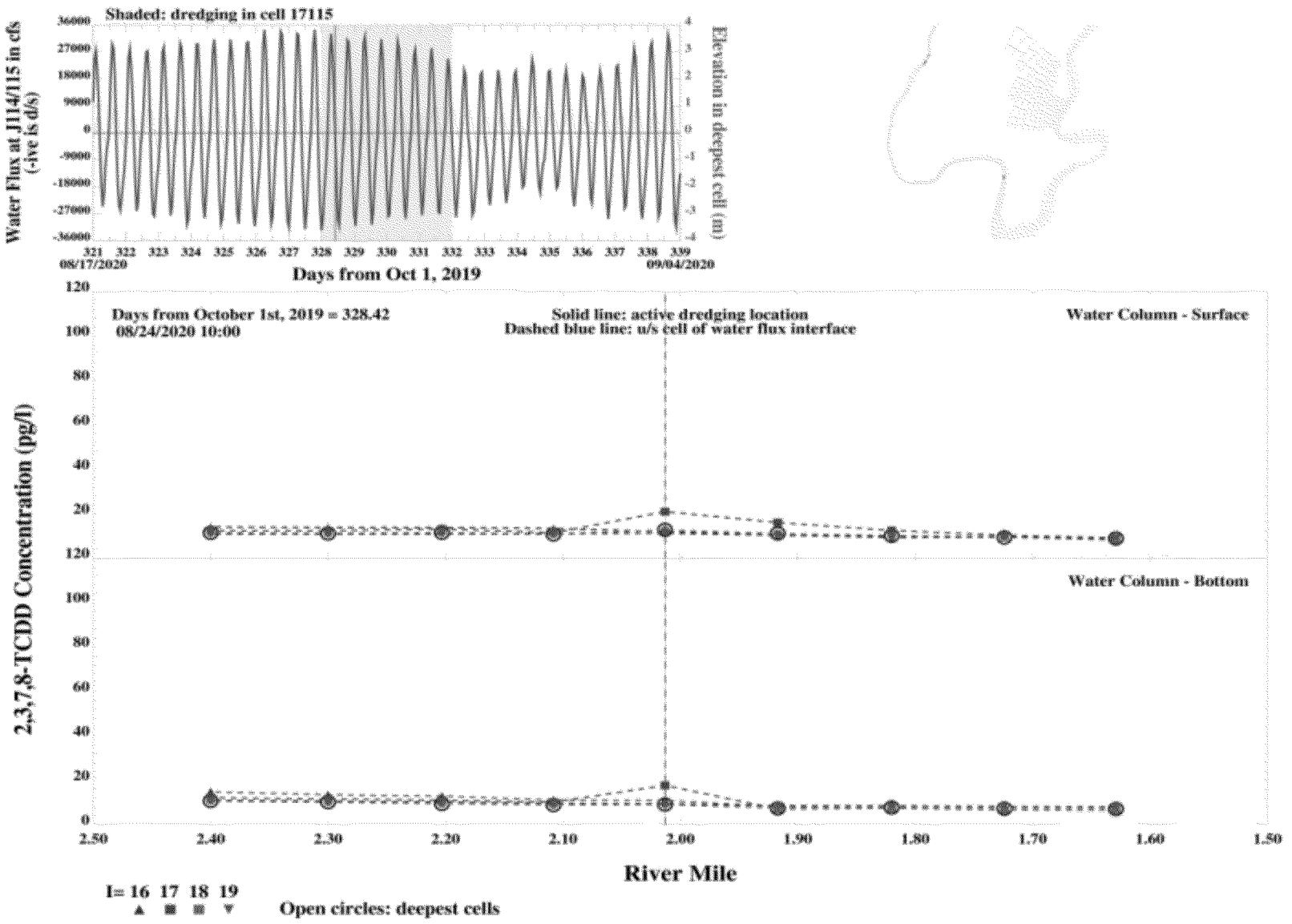

Spatial profile of 2,3,7,8-TCDD water column concentrations during dredging near RM 2 - spring tide - high slack tide

Figure 38

Lower 8.3 Miles of the Lower Passaic River

2016

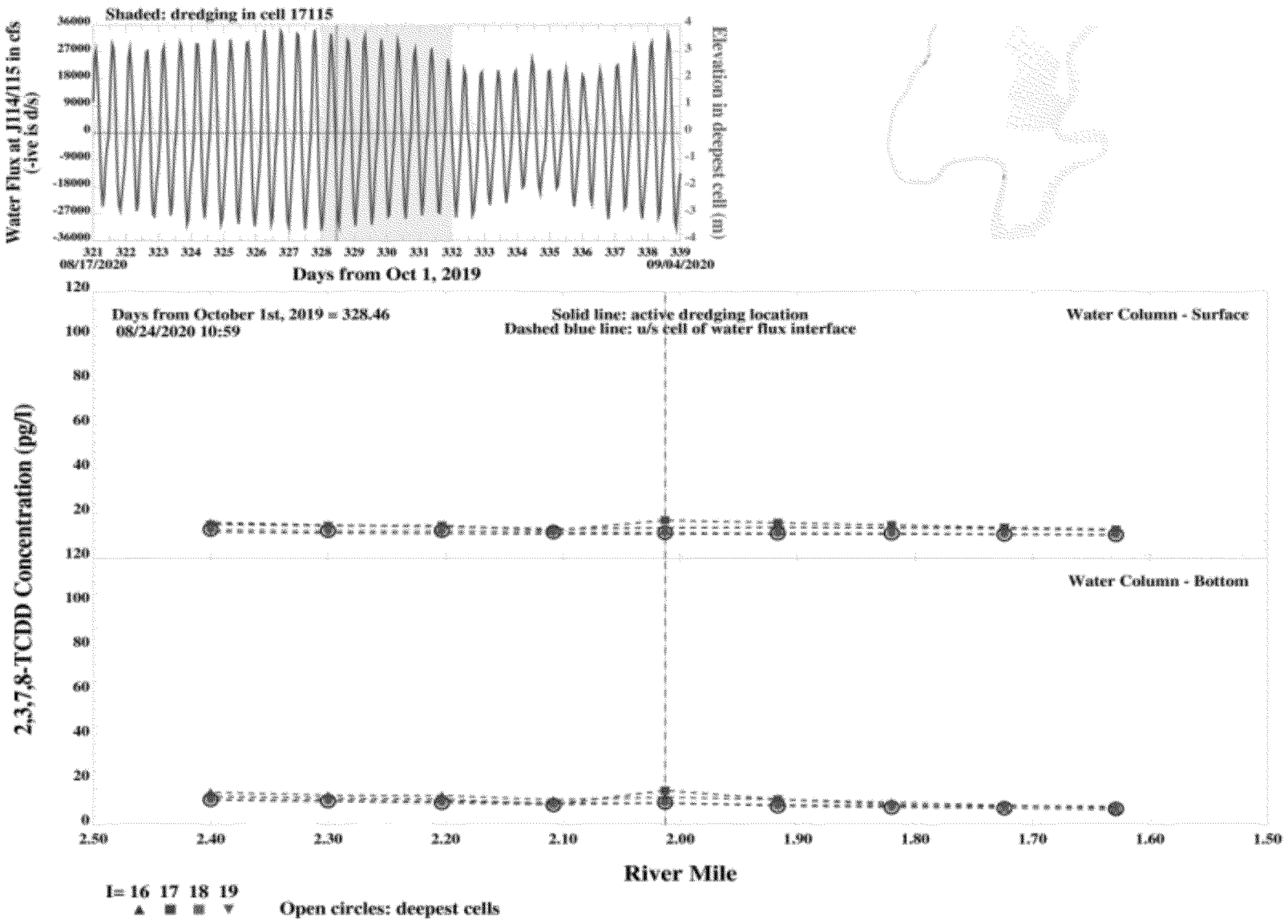

Spatial profile of 2,3,7,8-TCDD water column concentrations during dredging near RM 2 - spring tide - ebb tide 1 hour after high slack tide

Figure 39

Lower 8.3 Miles of the Lower Passaic River

2016

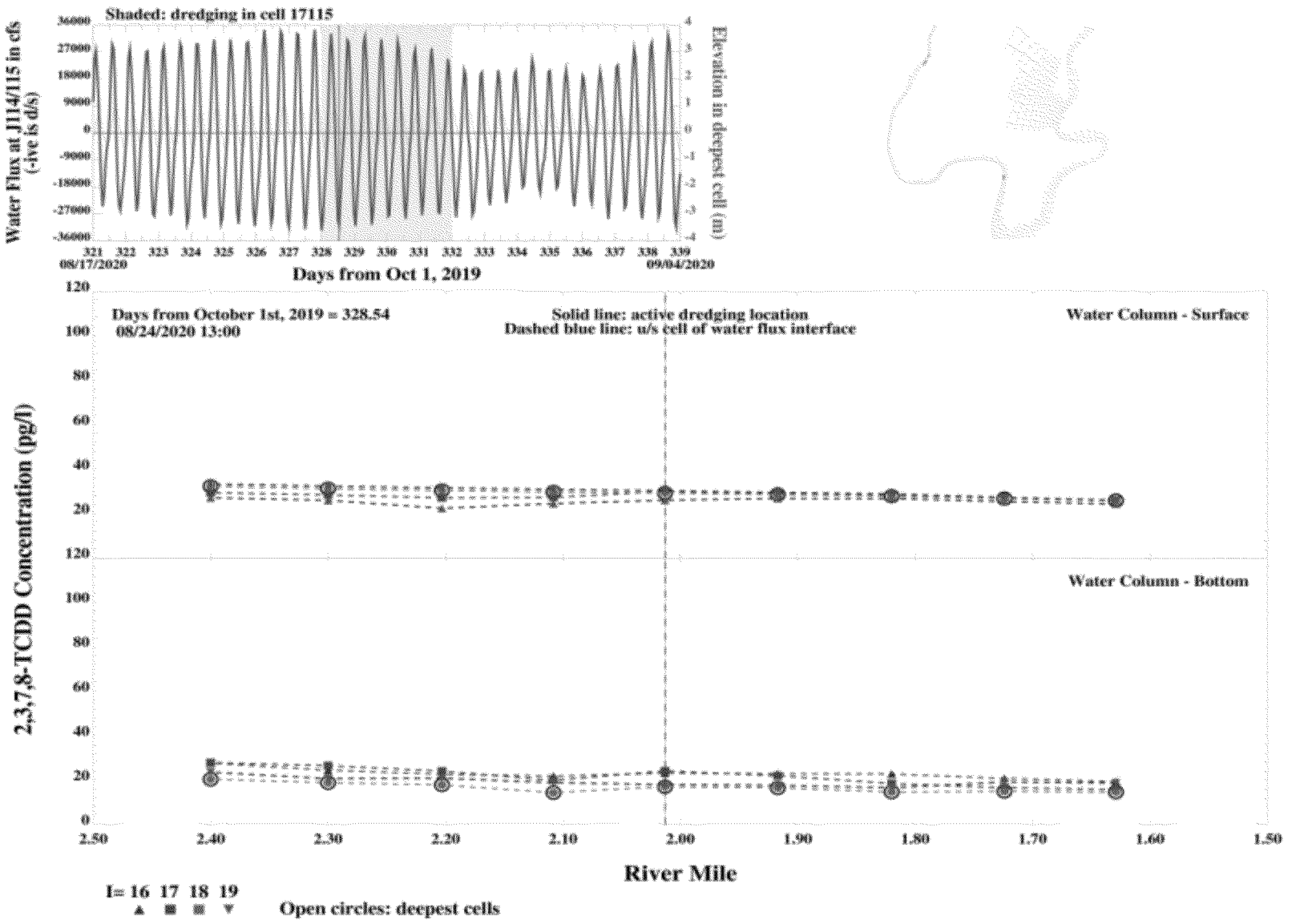

Spatial profile of 2,3,7,8-TCDD water column concentrations during dredging near RM 2 - spring tide - peak ebb tide

Figure 40

Lower 8.3 Miles of the Lower Passaic River

2016

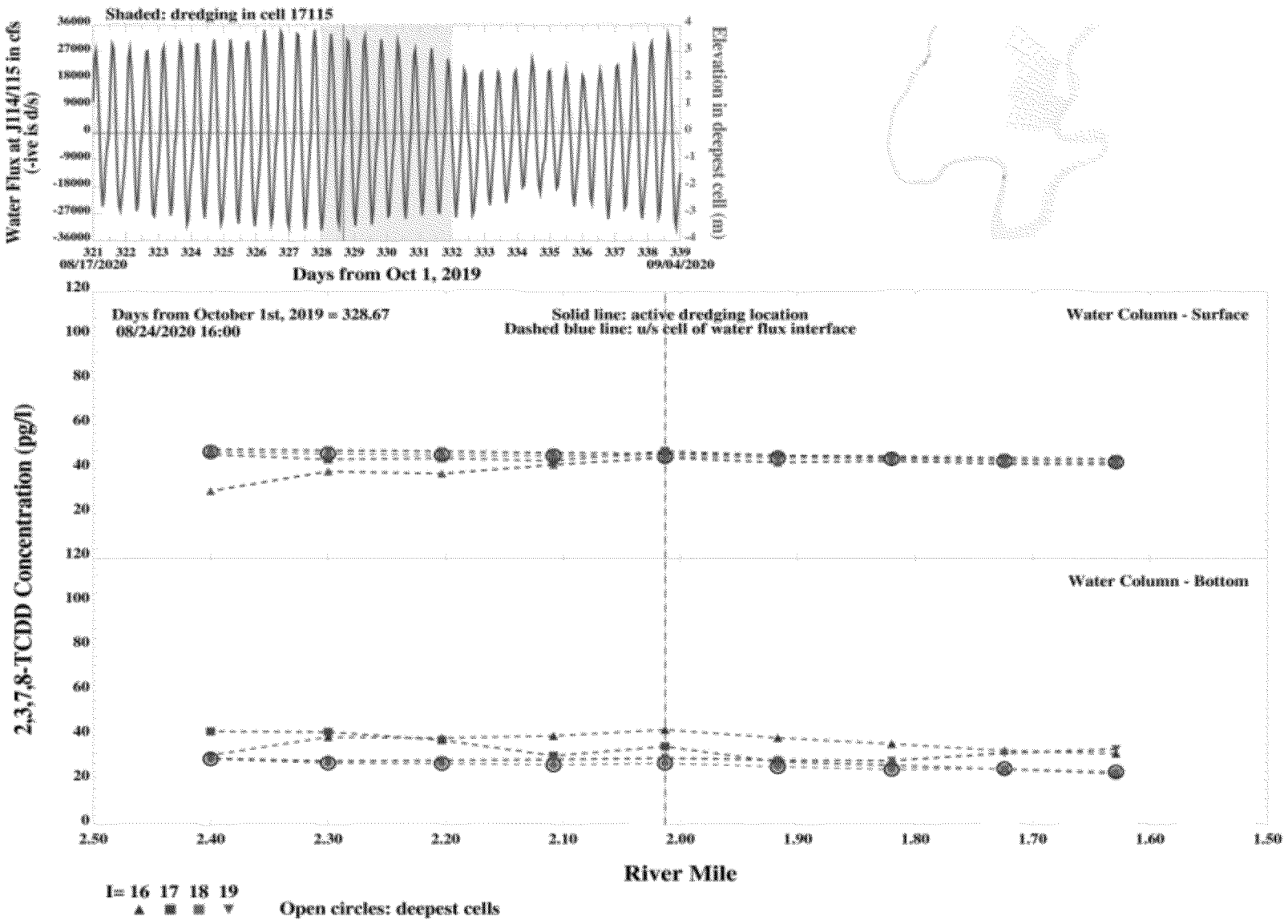

Spatial profile of 2,3,7,8-TCDD water column concentrations during dredging near RM 2 - spring tide - low slack tide

Figure 41

Lower 8.3 Miles of the Lower Passaic River

2016

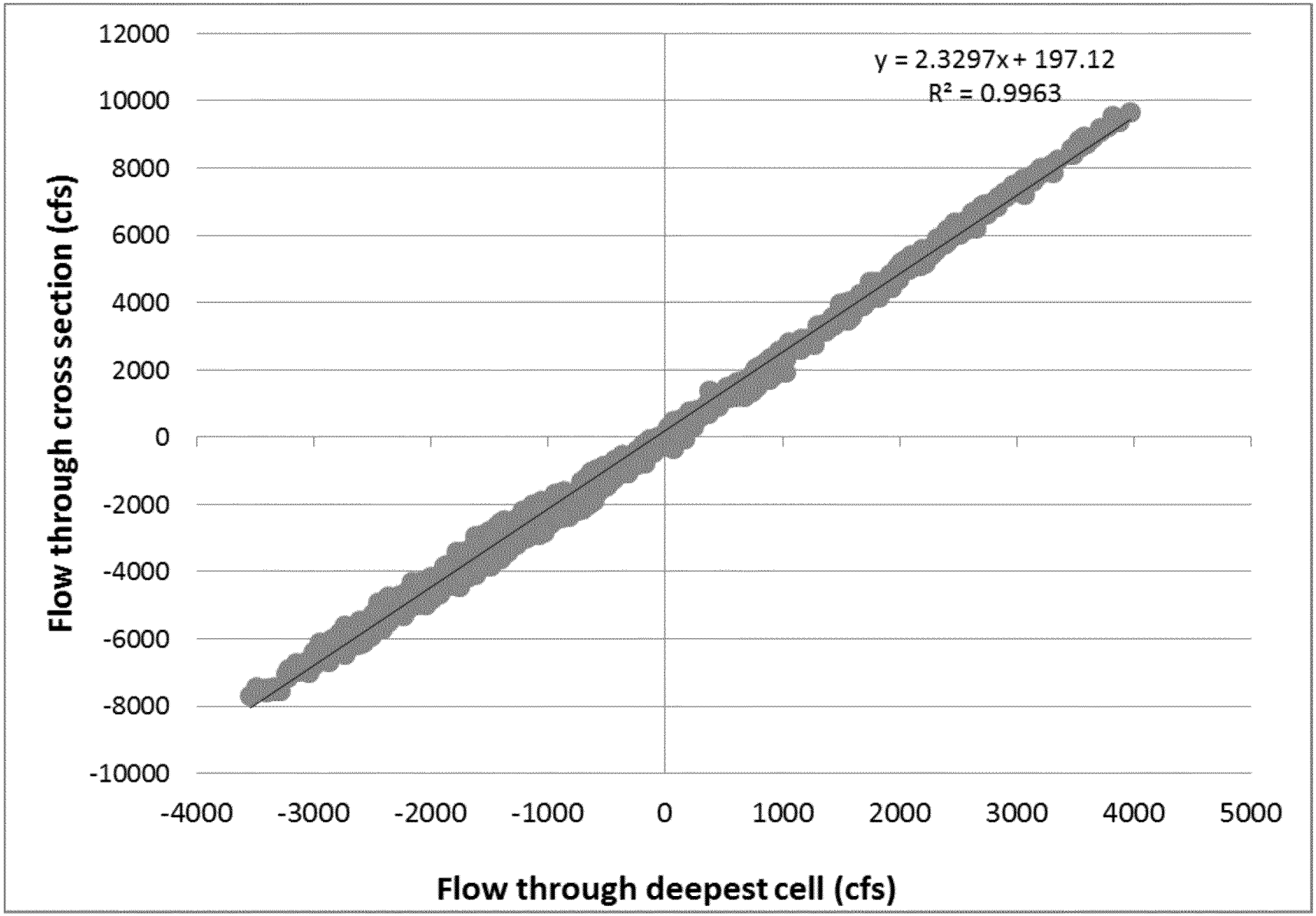

Flow through deepest cell vs flow through cross section for J=160 (River Mile 8.1)

Figure 42

Lower 8.3 Miles of the Lower Passaic River

2016

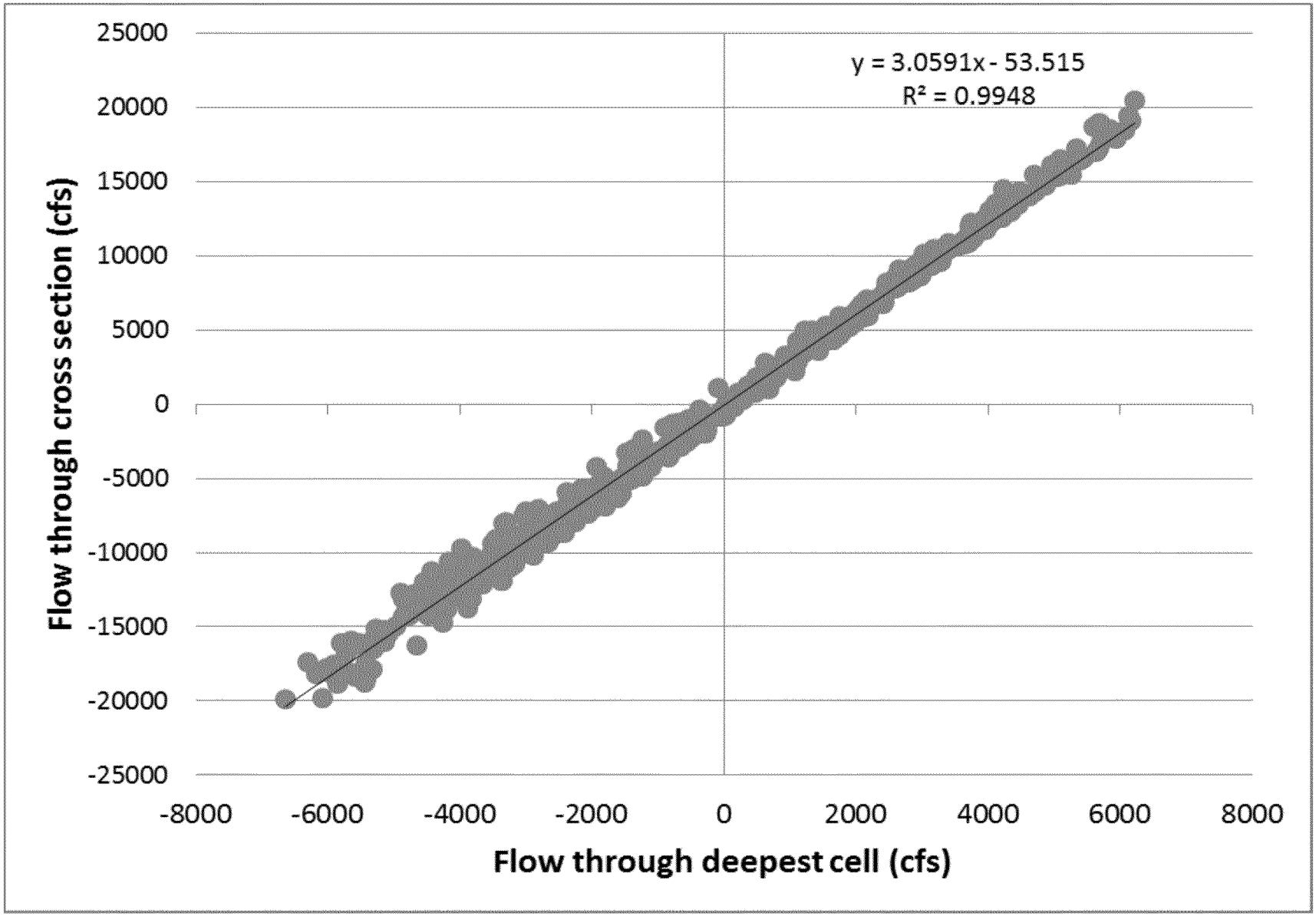

Flow through deepest cell vs flow through the cross section for J=106 (River Mile 1.2)

Figure 43

Lower 8.3 Miles of the Lower Passaic River

2016

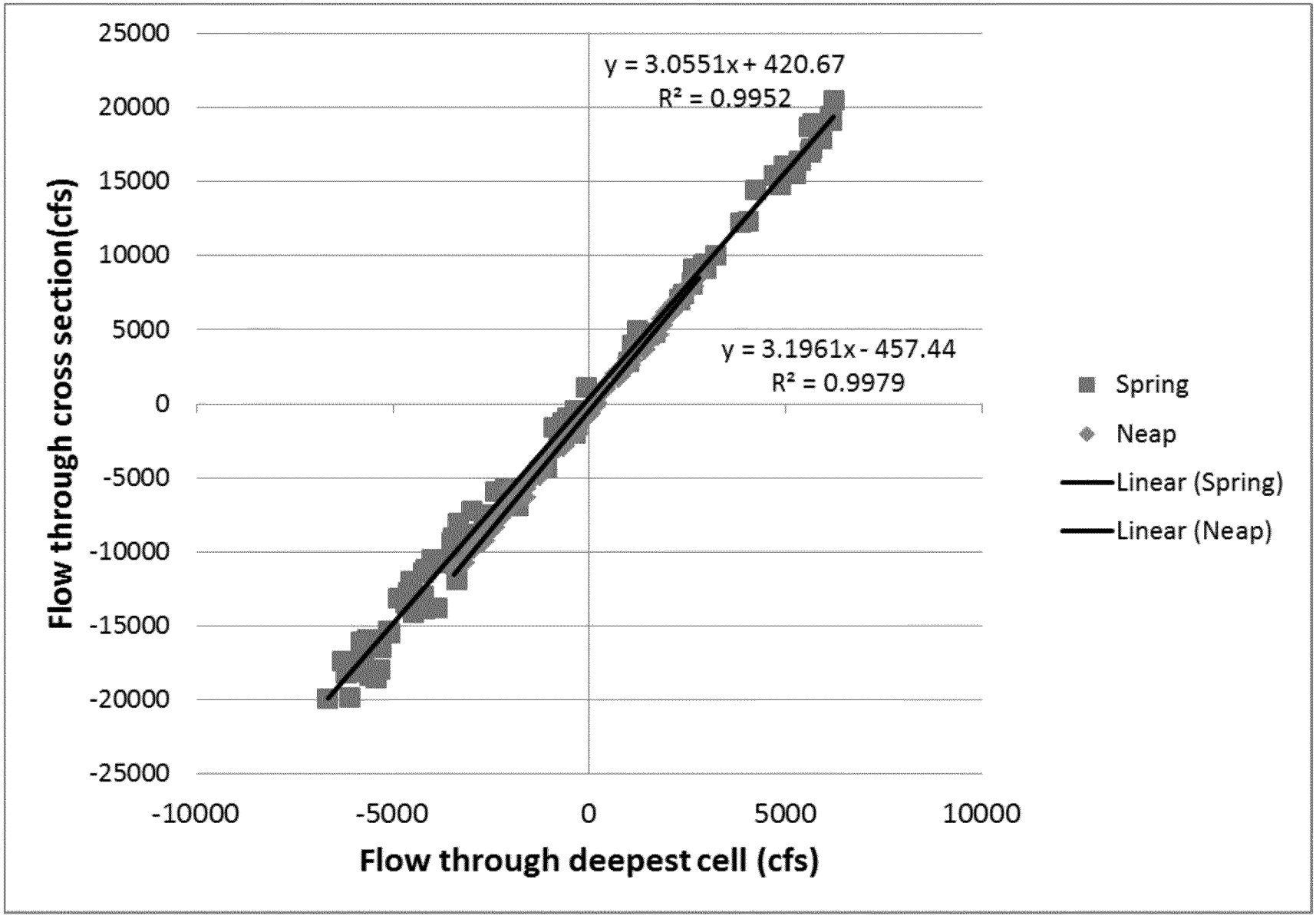

Flow through deepest cell vs flow through cross section for J=106 (River Mile 1.2) for a spring and neap period of the tidal cycle

Figure 44

Lower 8.3 Miles of the Lower Passaic River

2016

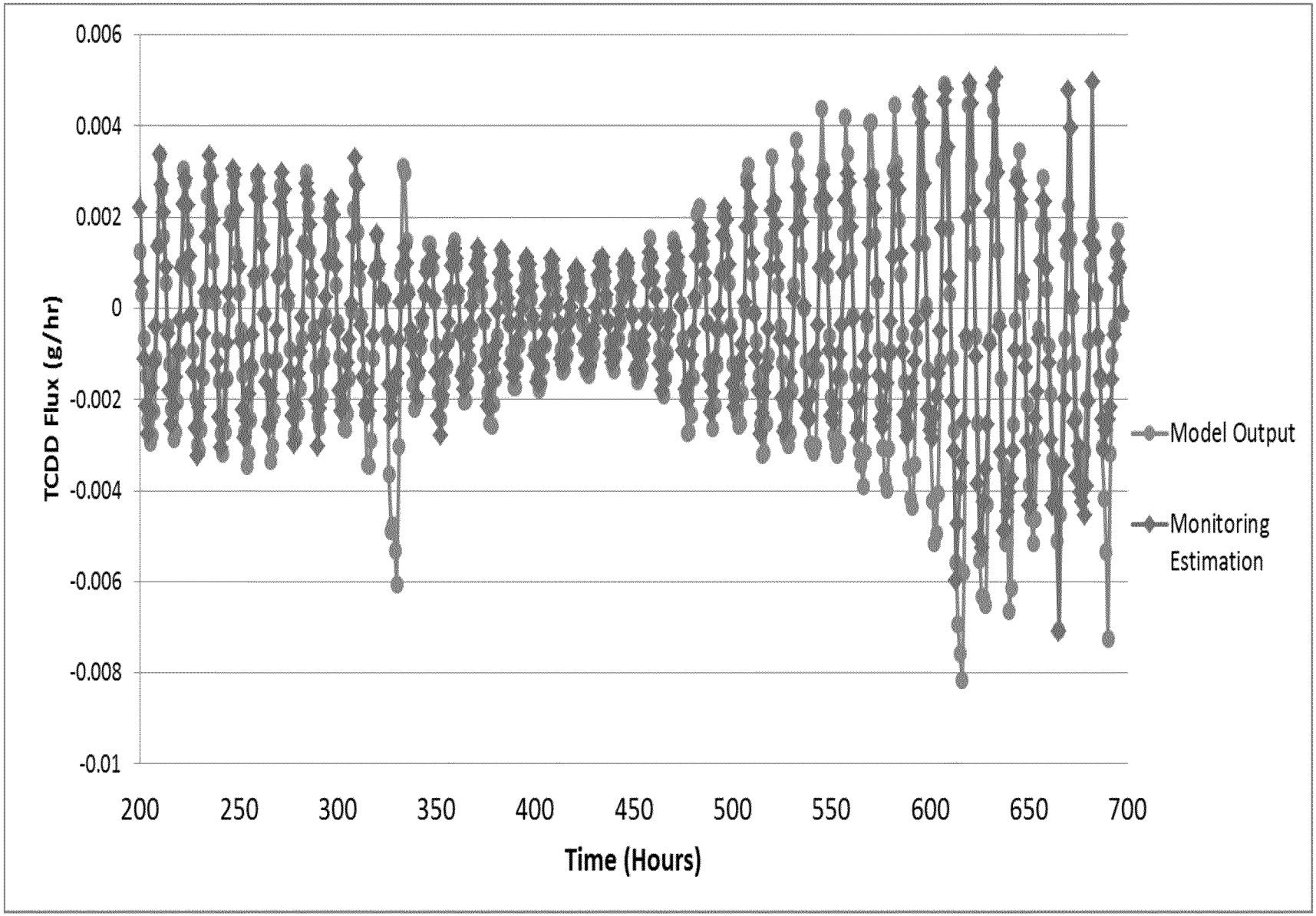

Estimation with periodic sampling (2 times per day, once each at peak ebb and flood) compared to model output

Figure 45

Lower 8.3 Miles of the Lower Passaic River

2016

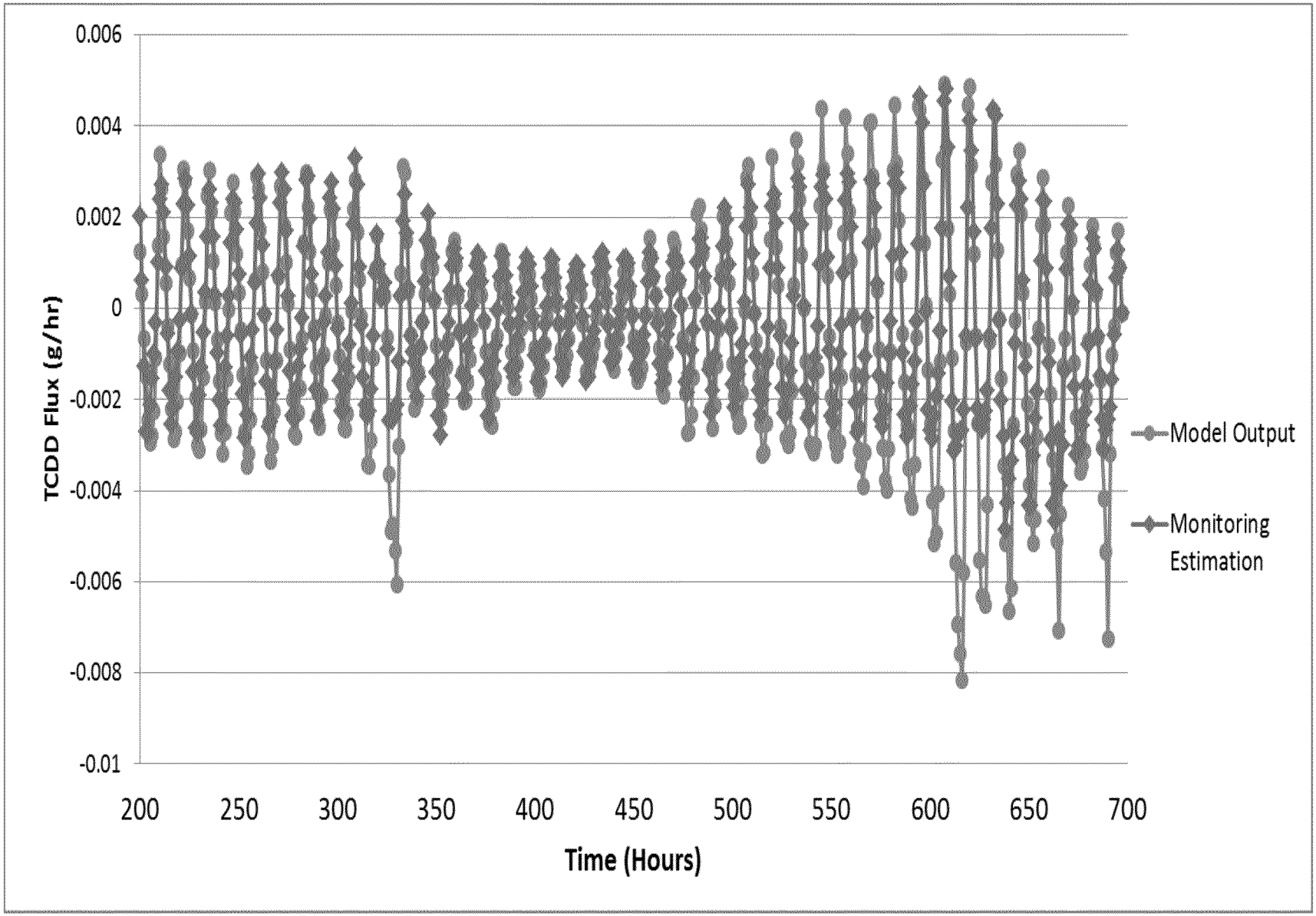

Estimation with periodic sampling (1 time per day, alternating peak ebb and flood) compared to model output

Figure 46

Lower 8.3 Miles of the Lower Passaic River

2016

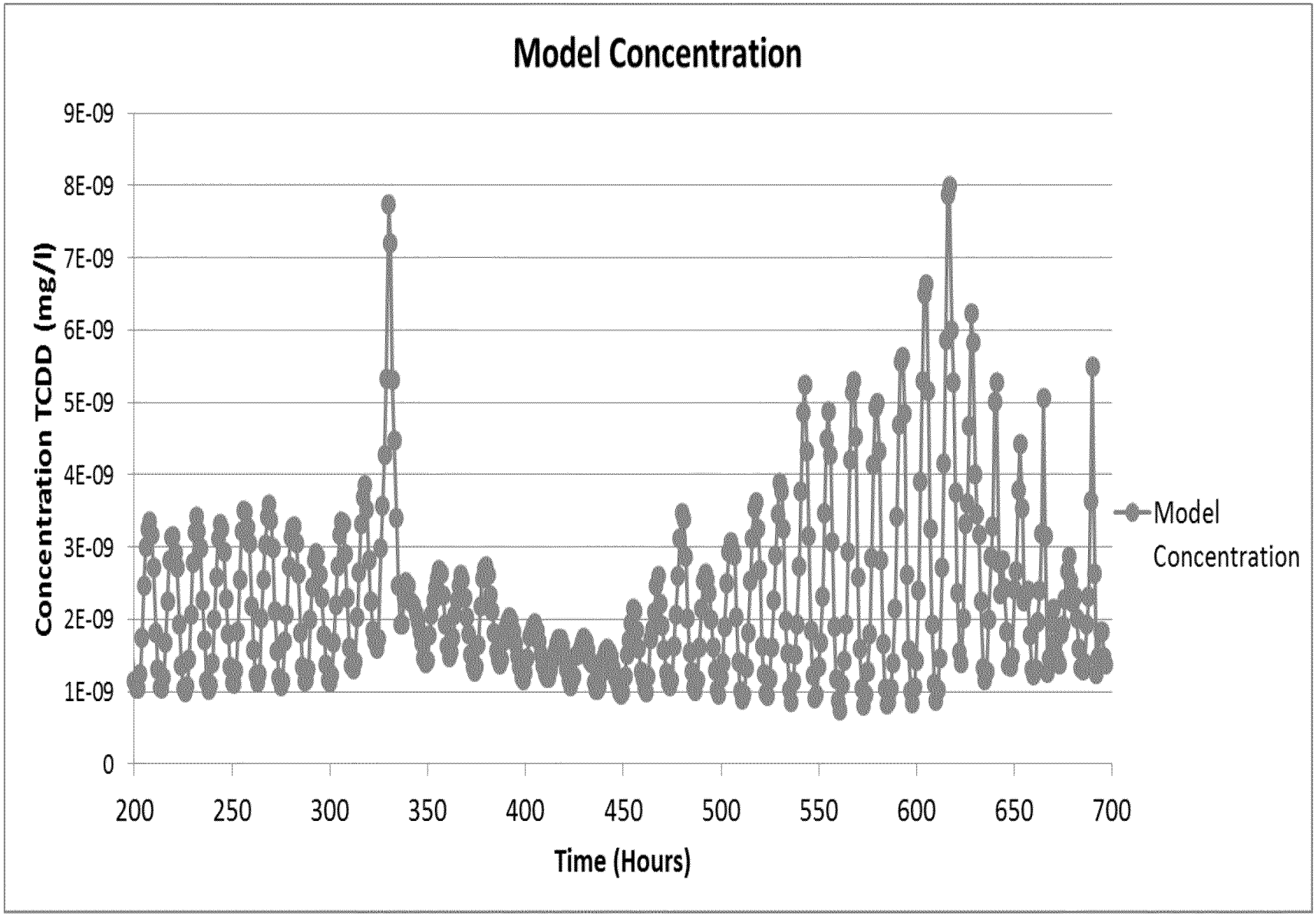

Model output of concentration

Figure 47

Lower 8.3 Miles of the Lower Passaic River

2016